University of California
Santa Barbara

A Survey of Characteristics and Signatures of A Few Low-Temperature Phases of Quantum Matter

A dissertation submitted in partial satisfaction
of the requirements for the degree

Doctor of Philosophy
in
Physics

by

Daniel Gregory Ish

Committee in charge:

Professor Mark Srednicki, Chair
Professor Cenke Xu
Professor David Weld

September 2018

The Dissertation of Daniel Gregory Ish is approved.

Professor Cenke Xu

Professor David Weld

Professor Mark Srednicki, Committee Chair

September 2018

A Survey of Characteristics and Signatures of A Few Low-Temperature Phases of Quantum Matter

by

Daniel Gregory Ish

For Sarah, partner and joy, and for Emmy, cat and role model.

Acknowledgements

First, I should acknowledge my collaborators. Mark Srednicki, Leon Balents, Cenke Xu, Matthew Fisher, Andreas Ludwig, Max Metlitski and Tim Hseih have all contributed significantly to my development as a physicist. Reaching back slightly further, I should also note that I would not have been able to succeed in graduate school without the mentorship of Barbara Jones and David Biron. I've also very much enjoyed and benefited from discussions with my classmates, particularly Alex Rassmussen and Kelly Pawlak.

On a personal level, I first and foremost have to acknowledge my (very soon to be) wife Sarah Del Ciello, who has been an incredible source of support during these years and without whom this thesis may never have happened. I should also thank my family, whose confidence in me and support for me have helped me to keep moving forwards. I'd also like to thank my roommates, Evan Bauer, Lucas Brady and Michael Swift, whose camraderie and discussion helped keep it light. Last, but certainly not least, I'd like to thank Darren "Chuck" Valovcin, for many helpful sidebars.

Curriculum Vitæ

Daniel Gregory Ish

Education

2018	Ph.D. in Physics (Expected), University of California, Santa Barbara.
2015	M.A. in Physics, University of California, Santa Barbara.
2013	B.S. in Mathematics with Honors, University of Chicago
2013	B.A. in Physics with Honors, University of Chicago

Publications

Ish, D. and Balents, L. "Theory of excitations and dielectric response at a spin-orbital quantum critical point," *PRB*, **92** 094413(2015).

L. Mittelstdt, M. Schmidt, Zhe Wang, F. Mayr, V. Tsurkan, P. Lunkenheimer, **D. Ish**, L. Balents, J. Deisenhofer, and A. Loidl. "Spin-orbiton and quantum criticality in $FeSc_2S_4$," *PRB* **91** 125112(2015)

Iwanir S; Tramm N; Nagy S; Wright C; **Ish D**; Biron D. "The microarchitecture of behavior during lethargus: homeostatic bout dynamics, a typical body posture, and regulation by a central neuron." Sleep. 2013;36(3):385-395.

Abstract

A Survey of Characteristics and Signatures of A Few Low-Temperature Phases of Quantum Matter

by

Daniel Gregory Ish

We study two distinct systems along a similar theme. In one, we present new theoretical studies of the optical properties of the J_2-λ model for the materieal $FeSc_2S_4$, which places it close to a quantum critical point on the disordered side of a quantum phase transition between a Néel ordered phase and a "Spin-Orbital Liquid" in which spins and orbitals are entangled, quenching the magnetization. We compute the dispersion relation for the quasiparticle excitations and the form of the collective response to electric field. We argue that the latter directly probes a low energy excitation continuum characteristic of quantum criticality, and that our results reinforce the consistency of this model with experiment. In the other, through a mixture of analytic and numerical techniques, we explore the optimal approximation by a free Majorana state to individual disorder realizations of the Sachdev-Ye-Kitaev model, along with a generalization of it. We elucidate the properties of the known time-reversal symmetry breaking phase in the generalized model, finding strong evidence of "spin glass" order. For the Sachdev-Ye-Kitaev model itself, our results are inconclusive but suggest a similar order may be present at $T = 0$.

Contents

Curriculum Vitae **vi**

Abstract **vii**

1 Introduction **1**
1.1 Permissions and Attributions 1
1.2 Context and Connective Tissue 1

2 Signatures of a Quantum Critical Paramagnet **8**
2.1 Introduction 8
2.2 Magnetic Dipole Exitations 11
2.3 Response to Electric Fields 21
2.4 Discussion 26

3 Instabilities of the Sachdev-Ye-Kitaev and Related Models **31**
3.1 Introduction 31
3.2 Formalism and Analytic Results 33
3.3 Numerical Results 48
3.4 Discussion 60

A Supplemental Calculations **64**
A.1 Derivatives of the Trial Free Energy 64
A.2 Specific Heat and Susceptibility Calculations 70

Bibliography **73**

Chapter 1

Introduction

1.1 Permissions and Attributions

1. The content of chapter 2 is the result of a collaboration with Leon Balents, and has previously appeared in Physical Review B[1].

2. The content of chaper 3 and Appendix A is the result of a collaboration with Mark Srednicki.

1.2 Context and Connective Tissue

The notion of a phase is a central organizing principle in condensed matter physics. For the sake of the uninitiated reader, we give a brief survey of the concept and its implications for experiment. The natural setting for discussing this question is the cannonical ensemble. Though we will primarily be concerned with these questions in quantum systems, we begin in a classical setting for the purposes of a gradual introduction of concepts. In this setting, we have some energy function for each classical state s, $E(s)$ and we assert that when the system is in thermal equilibrium at a temperature T the probability of

observing it in a state s is

$$p(s) \propto e^{-E(s)/k_B T} \tag{1.1}$$

Ostensibly for convinience, we form the free energy

$$\mathcal{F} = -k_B T \ln \left[\int e^{-E(s)/k_B T} \mathrm{d}s \right] \tag{1.2}$$

where what exactly we mean by this integral depends on the space of possible states. The convenience in question is that this allows us to easily write the probability of observing the system in state s as

$$p(s) = e^{-(E(s)-\mathcal{F})/k_B T} \tag{1.3}$$

and compute the expected value of any observable quantity as

$$\langle O(s) \rangle = \int O(s) p(s) \mathrm{d}s \tag{1.4}$$

Most commonly, one will be concerned with quantities which the energy depends on as

$$E(h, s) = E(0, s) - hO(s) \tag{1.5}$$

for some "applied field" h, which we imagine is under the control of the experimenter. In this instance, we can actually compute

$$\langle O(s) \rangle = -\frac{\partial \mathcal{F}}{\partial h} \tag{1.6}$$

along with higher cumulants using higher derivatives. This relationship is so useful that we will introduce artificial applied fields in order to compute any observables we desire. One can also immediately see that the bulk thermodynamic quantities that one might be interested in (i.e. average energy, entropy, specific heat, etc.) are also accessible via temperature derivatives of this free energy. This allows us the luxury of studying only the free energy, since it contains all of the information we are interested in.

We are now in a position to begin a roundabout definition of a phase. We start with a definition of a phase transition: a phase transition is what happens at a point of non-analyticity in the "thermodynamic limit" of the free energy (as a function of temperature and applied fields). Immediately, one is drawn to ask what exactly a "thermodynamic limit" is. For any model we study, there will be some parameter which characterizes the total size of the system at hand. This might be a number of discrete sites, N, or a total volume of the system, V. For the sake of concreteness,[1] let us take the case where the state space is discrete and equipped with the counting measure, giving a total number of states which is some well behaved function of a number of sites N. Thus, the free energy becomes the log of a finite sum of exponentials and (provided the energy function is analytic in applied fields) is analytic everywhere. In order to observe a non-analyticity, we must take the system size to ∞ at fixed values of the applied fields and temperature. Taking this limit is referred to as the "thermodynamic limit."

With this in hand, we say vaguely that phases are the regions of parameter space separated by phase transitions. One might reasonably ask what is vague about that definition. We illustrate the limitations with an example. Consider the $d = 2$ classical Ising model. The state space of the model is $\mathbb{Z}_2^{N^2}$, thought of as N^2 "signs" $\sigma_{i,j}$ sitting

[1] One could no doubt reformulate this argument in a more universal context using the Vitali convergence theorem, but the effort is disproportionate to the impact for our purposes.

on an $N \times N$ grid. That is, to be pedantic

$$\sigma_{i,j} = \pi_{i+Nj}(s) \tag{1.7}$$

for $s \in \mathbb{Z}_2^{N^2}$ where π_k is the projection onto the kth coordinate and we are thinking of $\mathbb{Z}_2$ as $(\{\pm 1\}, \cdot)$. The measure on the state space, $\mathrm{d}s$, is the counting measure, i.e. the integral is actually a sum. The energy function is given by

$$E(s) = -\frac{J}{2} \sum_{i=1}^{N} \sum_{\nu=\pm 1} \sigma_{i,j}\sigma_{i,j+\nu} + \sigma_{i,j}\sigma_{i+\nu,j} - \sum_{i} h_{i,j}\sigma_{i,j} \tag{1.8}$$

where all arithmetic in subscripts is carried out mod N. Onsager[2] solved this model exactly at $h_{i,j} = 0$, showing that the $N \to \infty$ limit of the free energy has a non-analyticity as a function of T at

$$T = T_c \equiv \frac{2J}{k_B \ln(1 + \sqrt{2})} \tag{1.9}$$

Thus, by our definition we are drawn to conclude that this model exhibits two phases, one above and one below this temperature. The question of what sets these two phases apart from one another (i.e. how are they different physically) is closely related to the foreshadowed deficiency in our current definition.

First, we address the deficiency in our definition of a phase. Consider the model at $h_{i,j} = h$, where h is not necessarily 0. Using the more modern tool of the renormalization group[3], one can show that actually the free energy as a function of both h and T is analytic everywhere except the line $h = 0, T \leq T_c$. This poses a rather dramatic problem for our definition, as the points of non-analyticity do not separate regions in parameter space. Furthermore, one wonders at the apparent change in number of phases with the addition of a new parameter.

We solve these problems by defining a phase and a phase transition in a somewhat narrower context, motivated by what exactly happens in the Ising model at $h_{i,j} = 0$ and $T = T_c$. In the case of the Ising model, we can notice that the model has a $\mathbb{Z}_2$ symmetry at $h_{i,j} = 0$ given by

$$s \to -s \tag{1.10}$$

Demanding that this $\mathbb{Z}_2$ symmetry be preserved restricts us to the $h_{i,j} = 0$ line in parameter space and allows this non-analyticity to actually separate two distinct regions. This gives us a more serviceable definition of a phase transition: if a model has a symmetry group G, a phase transition is a non-analyticity in the free energy in the absence of any applied fields which break the symmetry.

Of course, what constitutes an "applied field" rather than a inextricable portion of one's model is intertwined with the question of what symmetries one's model possesses. In practice, this ambiguity is most frequently resolved in one of two ways, depending on the goals of the inquiry. If one is motivated by understanding an actual physical system, then the properties of that system will answer this question. That is, if it's a field the experimenter is applying, it's probably an applied field. On the other hand, if one is motivated to explore possible classes of phase transitions, one is free to specify the symmetry of the model at will.

At first blush, the symmetry group in question seems a bit superfluous, since we may as well have simply declared some fields "off limits" in an only marginally more ad-hoc way. However, the symmetry group that the model possesses is actually closely linked with the nature of the transition. Let us return to the $d = 2$ Ising model with $h_{i,j} = h$.

One can define a magnetization:

$$m(h,T) = \frac{1}{N^2}\sum_{ij}\langle\sigma_{i,j}\rangle \tag{1.11}$$

and notice that the action of $\mathbb{Z}_2$ that gives a symmetry at $h = 0$ also gives

$$m(-h,T) = -m(h,T) \tag{1.12}$$

In terms of this quantity, the non-analyticity at $h = 0$, $T < T_c$ is fairly easy to characterize. We can notice that

$$\lim_{h\to 0^+}\lim_{N\to\infty} m(h,T) = m_s \neq 0 \tag{1.13}$$

and of course the limit from below is equal to $-m_s$, according to Equation 1.12. We refer to m_s as the "spontaneous magnetization," since it appears as a residual magnetization even at $h = 0$. Since we can see that

$$m(h,T) = -\frac{1}{N^2}\frac{\partial\mathcal{F}}{\partial h} \tag{1.14}$$

in concert with Onsager's calculation, this indicates that the non-analyticity in the free energy on this line is due to a jump discontinuity in the h derivative of the free energy.

We now have three different candidates for the $h = 0$ state of the system depending on our order of limits and which direction we approach $h = 0$ from in the thermodynamic limit. Since two of these have some spontaneous magnetization which breaks the $\mathbb{Z}_2$ symmetry according to the direction of approach, we think of the symmetry as having been broken in the thermodynamic limit. Practically speaking, we use these two states to model the state of a physical system due to the probability that any physical system

will have encountered some transient biasing field during its preparation.

In the remaining chapters, we will explore two systems of considerably greater complexity that nonetheless develop along this theme. In one, we find a system in the ordered side of a transition which breaks crystallographic T_d and translations symmetries and find some experimental evidence for the proximity of this transition. In the other, a simple $\mathbb{Z}_2$ symmetry breaking will interact interestingly with disorder, giving a richer ordered state.

Chapter 2

Signatures of a Quantum Critical Paramagnet

2.1 Introduction

A suite of experimental probes[4, 5, 6, 7, 8, 9, 10] identifies the A-site spinel $FeSc_2S_4$ as a rare example of a orbitally degenerate antiferromagnet which resists magnetic or orbital order down to a temperature of tens of millikelvin, making it a truly quantum paramagnet. It has been suggested[11, 12] to lie close to a quantum critical point, making it a compelling object of study. This prior theoretical work proposed the "J_2-λ" model for this compound in terms of spin two, $\mathbf{S}_j$, and spin one half, $\mathbf{T}_j$, operators on the diamond lattice with the Hamiltonian

$$H = J_2 \sum_{\langle i,j \rangle} \mathbf{S}_i \cdot \mathbf{S}_j + \sum_i \mathcal{H}_i^0 - B \sum_i S_i^z \tag{2.1}$$

where $\langle i,j\rangle$ stands for next nearest neighbor bonds and the on-site Hamiltonian $\mathcal{H}_i^0$ is given by

$$\mathcal{H}_i^0 = -\frac{\lambda}{3}\left(\sqrt{3}T_i^x\left[(S_i^x)^2-(S_i^y)^2\right]+T_i^z\left[3\,(S_i^z)^2-\mathbf{S}_i^2\right]\right) \tag{2.2}$$

with $J_2>0$ and $\lambda>0$. We have included in Eq. (2.1) an external magnetic field B, taken for concreteness along the crystalline (001) axis, whose effects we will study further in the following. One should interpret this Hamiltonian as describing the low-energy dynamics of the 6 d electrons on the Fe^{2+} sites. Due to the tetrahedral crystal field, the d manifold splits into a lower e doublet and an upper t_2 triplet. These states are then filled in a high-spin configuration on the assumption that on site Hund's Rule exchange dominates the crystal field splitting, giving an overall spin 2 ($\mathbf{S}_i$) together with a two fold orbital degeneracy ($\mathbf{T}_i$). The J_2 term in the Hamiltonian is a NNN antiferromagnetic exchange term which arises in the standard way from virtual hopping between Fe^{2+} sites and the λ term represents the effect of spin-orbit coupling at second order, coupling the e hole to the overall spin 2.[13, 14]

With $J_2 = B = 0$, $\mathcal{H}_i^0$ describes a system of uncoupled Fe^{2+} sites with tetrahedral geometry under the influence of spin orbit coupling. This splits the 10-fold degenerate high-spin manifold into five equally spaced levels separated by energy λ. These are, in order of ascending energy, an a_1 singlet, a t_1 triplet, an e doublet, a t_2 triplet and an a_2 singlet. The a_1 ground state takes the form

$$\frac{1}{\sqrt{2}}\left|x^2-y^2\right\rangle|0\rangle+\frac{1}{2}\left|3z^2-r^2\right\rangle(|2\rangle+|-2\rangle) \tag{2.3}$$

where the number in the second ket in each product refers to the S^z eigenvalue. Critically, this state has zero average magnetization along all axes. In the presence of J_2,

single site t_1 excitations ("triplons" or "spin-orbitons") acquire a $\mathbf{k}$-dependent dispersion, but remain massive until $J_2/\lambda = 1/16$ at which point the system undergoes a quantum phase transition to antiferromagnetic ordering at wave vector $\mathbf{q} = (2\pi, 0, 0)$ and symmetry related wave vectors.[11, 12] In the J_2-λ model, this ordering actually happens independently on each of the fcc sublattices. A NN exchange term, J_1, is also allowed by symmetry,[11, 12] but is expected to be much smaller[11, 12, 15] and is difficult to distinguish from J_2 experimentally at $\mathbf{k} = 0$, which will be the regime of focus in this article. This term controls the relative orientation of the magnetizations of the A and B sublattices.

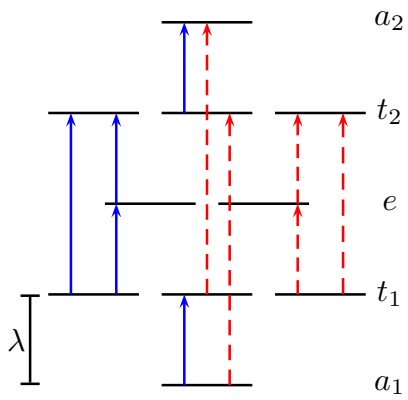

Figure 2.1: Spectrum of $\mathcal{H}_i^0$, with magentic dipole allowed transitions (blue) and electric dipole allowed transitions (red, dashed). The number of lines in a level indicates the degeneracy of that level.

One can argue for the consistency of this model with $FeSc_2S_4$ at lowest order in terms of two distinctive experimental observations: the lack of observed magnetic ordering down to temperatures of 50mK[9, 10] and the observation of a low energy mode at momentum $(2\pi, 0, 0)$ by neutron scattering.[8] Taken together, these suggest that the model at least qualitatively predicts the behavior of the compound if we suppose that the compound lies on the disordered side of the transition close to the QCP. Indeed, previous estimates[11, 12] of the magnitude of J_2/λ in $FeSc_2S_4$ give $J_2/\lambda \approx 1/17$, putting

the material just on the disordered side of the transition.

Given the striking properties of this material, it is no surprise that it has been the subject of recent experimental investigations, primarily focused on its optical properties.[4, 5] In this article, we attempt to make contact between this model and the observed optical properties of $FeSc_2S_4$ in order to argue for its continued consistency with experimental results. In order to do this, we will both investigate the fate of single site dipole allowed transitions in the presence of non-zero J_2, predicting both the shift in location and g factor, and investigate the character of the collective response to $\mathbf{k} = 0$ electric fields. We also derive expressions for as-yet unobserved quantities and propose possible experiments to measure them.

2.2 Magnetic Dipole Exitations

The single site problem has a single magnetic dipole allowed transition from the ground state, $a_1 \to t_1$. We expect that in the presence of J_2, this excitation will still result in a peak in the AC response of the material to magnetic fields, but will shift in energy. Given the proposed proximity of the material to a quantum phase transition, we expect perturbation theory to be inaccurate when predicting the location of these excitations. Thus, to determine their dispersion, we calculate the RPA susceptibility in the presence of a (001) directed field and investigate its pole structure as a function of $\mathbf{k}$.

2.2.1 Formalism and $B = 0$ Magnetic Dipole Excitations

To that end, we consider the imaginary time dynamic susceptibility

$$\chi_{ij}^{\mu\nu}(\tau_1 - \tau_2) = \left\langle T_\tau \mathcal{S}_i^\mu(\tau_1)\mathcal{S}_j^\nu(\tau_2)\right\rangle \tag{2.4}$$

where

$$\mathcal{S}^{\mu}(\tau) = S^{\mu}(\tau) - \langle S^{\mu} \rangle \tag{2.5}$$

Performing a Hubbard-Stratonovich transformation to decouple the exchange term, we find the partition function to be given by

$$Z = \int \mathcal{D}[\Phi] e^{-S_{eff}[\Phi]} \tag{2.6}$$

with the effective action for the auxiliary field Φ

$$S_{eff}[\Phi] = \frac{1}{2} \int \mathrm{d}\tau \sum_{ij} J_{ij}^{-1} \Phi_i \cdot \Phi_j - \ln W[\Phi] \tag{2.7}$$

where $W[\Phi]$ is the partition function for the $J_2 = 0$ problem with a magnetic field of $-i\Phi^{\mu}\mathbf{e}^{\mu}$ applied to each site (the "single site" problem). The dynamic susceptibility is then related to the propagator for the auxiliary field, $\Omega(\mathbf{k}, \omega)$, by

$$\chi(\mathbf{k}, \omega) = J(\mathbf{k})^{-1} - J(\mathbf{k})^{-2} \Omega(\mathbf{k}, \omega) \tag{2.8}$$

where $J(\mathbf{k})$ is the Fourier transform of the interaction

$$J(\mathbf{k}) = J_2 \sum_{\mathbf{A}} \cos\left(\mathbf{k} \cdot \mathbf{A}\right) \tag{2.9}$$

with $\mathbf{A}$ the 12 fcc nearest neighbors. If we then expand the action to second order in Φ about its saddle point ($\Phi = 0$), we find that the bare propagator for the auxiliary field,

Ω_0, is given by

$$\Omega_0 = [J(\mathbf{k})^{-1} + \chi_0(\omega)]^{-1} \tag{2.10}$$

with $\chi_0(\omega)$ the dynamic susceptibility of the single site problem and the inverse being, of course, the matrix inverse. Together with Equation 2.8 this gives the RPA susceptibility

$$\chi_{RPA}(\mathbf{k}, \omega) = \chi_0(\omega)[1 + J(\mathbf{k})\chi_0(\omega)]^{-1} \tag{2.11}$$

which we analytically continue to extract the real-time RPA susceptibility in terms of the real-time single site susceptibility. We can write the real time single site susceptibility in terms of the spectral representation

$$\chi_0^{\mu\nu}(\omega) = \sum_{j \neq 0} \frac{\langle 0|S^\mu|j\rangle \langle j|S^\nu|0\rangle}{E_j - E_0 - \omega} + \frac{\langle 0|S^\nu|j\rangle \langle j|S^\mu|0\rangle}{E_j - E_0 + \omega} \tag{2.12}$$

with $|0\rangle$ denoting the ground state. Using this, we find that both the single site and RPA susceptibilities are multiples of the identity and that the RPA susceptibility exhibits poles at

$$\omega(\mathbf{k}) = \lambda\sqrt{1 + \frac{4}{\lambda}J(\mathbf{k})} \tag{2.13}$$

which predicts a pole in the $\mathbf{k} = 0$ susceptibility at

$$\omega(\mathbf{0}) = \lambda\sqrt{1 + 48\frac{J_2}{\lambda}} \approx 1.95\lambda \tag{2.14}$$

at the predicted value for J_2, $J_2 = \lambda/17$, as previously reported.[11] Expanding this dispersion to first order in J_2 gives

$$\omega(\mathbf{k}) = \lambda + 2J(\mathbf{k}) + O(J_2^2) \tag{2.15}$$

in agreement with first order perturbation theory.

2.2.2 Magnetic Dipole Excitations with $B \neq 0$

The preceding analysis can be repeated in the presence of a magnetic field with little change. The location of the Φ saddle point simply shifts due to the presence of a magnetic term in the associated single site problem, leading to a different mean field. The new saddle point is of the form

$$\Phi_0(\tau) = -i\beta^\mu \tag{2.16}$$

with β^μ determined by the mean field consistency equation

$$\beta^\mu = 12J_2 \langle S^\mu \rangle_0 \tag{2.17}$$

where $\langle\cdot\rangle_0$ stands for averages taken in the single site problem in the presence of the field $(B^\mu - \beta^\mu)\,\mathbf{e}^\mu$, with $B^\mu\mathbf{e}^\mu$ the applied field. In our case, since the applied field is considered only along the (001) direction, we have that only β^z is non-zero. The form of the RPA susceptibility is the same as in Equation 2.11, save for the fact that the single site susceptibility is now calculated in the mean field

$$\chi_0^{\mu\nu}(\tau) = \langle T_\tau \mathcal{S}^\mu(\tau)\mathcal{S}^\nu(0)\rangle_0 \tag{2.18}$$

Applying the magnetic field reduces the tetrahedral symmetry of the single site problem, causing some transitions $a_1 \to t_2$ to become allowed. As will be discussed in Section 2.3, the shifts in the energies of the t_2 excitations may not be well captured by the the J_2-λ model and have not yet been experimentally observed. In the analysis that follows, the poles due to these transition exhibit some pathological behavior. In particular, as $B \to 0$, they return to the single site energy of the t_2 excitations, in contrast with the behavior of the t_1 excitations. This is also in contrast to the perturbative result, which gives a shift of the t_2 energies at second order in J_2. Consequently, we will not present the results of the $B \neq 0$ RPA for the two t_2 excitations that become allowed.

For $B \neq 0$, the analysis of the pole structure of the RPA suceptibility is complicated significantly by that fact that the single site susceptibility is no longer a multiple of the identity. We only retain that the susceptibility is block-diagonal in the zz and xy blocks. Even with this reduced symmetry, there is still some remaining structure that we can exploit. Using the spectral representation, we see that $\chi_0^{xx} = \chi_0^{yy}$ and $\chi_0^{xy} = -\chi_0^{yx}$. Together with the fact that χ_0^{yx} is purely imaginary, this implies that the single site susceptibility is diagonalized at all frequencies (and hence all imaginary times) by the same unitary transformation. The eigenvalues of the xy single site susceptibility are then

$$\chi_0^{\pm}(\tau) = \chi_0^{xx}(\tau) \pm i\chi^{xy}(\tau) = \frac{1}{2}\left\langle T_\tau S^{\mp}(\tau) S^{\pm}(0)\right\rangle_0 \tag{2.19}$$

and, of course, χ^{zz}. Together with Equation 2.11, gives that the eigenvalues of the RPA susceptibility are

$$\chi_{RPA}^{\pm}(\mathbf{k},\omega) = \frac{\chi_0^{\pm}(\omega)}{1 + J(\mathbf{k})\chi_0^{\pm}(\omega)} \tag{2.20}$$

and

$$\chi^{zz}_{RPA}(\mathbf{k},\omega) = \frac{\chi^{zz}_0(\omega)}{1 + J(\mathbf{k})\chi^{zz}_0(\omega)} \tag{2.21}$$

Furthermore, we can actually see by the spectral representation that $\chi^-_0(\omega) = \chi^+_0(-\omega)$, which implies the same result for χ^-_{RPA}. So, we actually need only investigate the pole structure of χ^+_{RPA} and χ^{zz}_{RPA}. This is quite easy to do for χ^{zz}, since only one state has a non-vanishing S^z matrix element with the ground state at all B. Calling this state $|z\rangle$ and its energy ϵ_z, we find poles of χ^{zz}_{RPA} at

$$\omega_z(\mathbf{k}) = \epsilon_z \sqrt{1 + \frac{2J(\mathbf{k})}{\epsilon_z} |\langle 0|\mathcal{S}^z|z\rangle|^2} \tag{2.22}$$

where it should be noted that ϵ_z, $|0\rangle$, $|z\rangle$ and $\mathcal{S}^z$ all depend on B through the mean field. This result can also be seen to be consistent with perturbation theory to first order in J_2, though one must carefully track the dependence of the mean field on J_2 in order to obtain all the terms.

The poles of χ^+_{RPA} are more difficult to extract exactly, due to the larger number of states contributing to χ^+_0. We can cast their location as the roots of an 8th order polynomial, however, and solve this polynomial numerically as a function of B and J_2, producing Figures 2.2 and 2.3. Notice that non-zero J_2 actually reinforces the linear behavior of the triplet at $\mathbf{k} = 0$ in small field. This is easily understood by noticing that the mean field is strictly smaller than the applied field, since the antiferromangetic interaction imposes an energy cost to uniform magnetization.

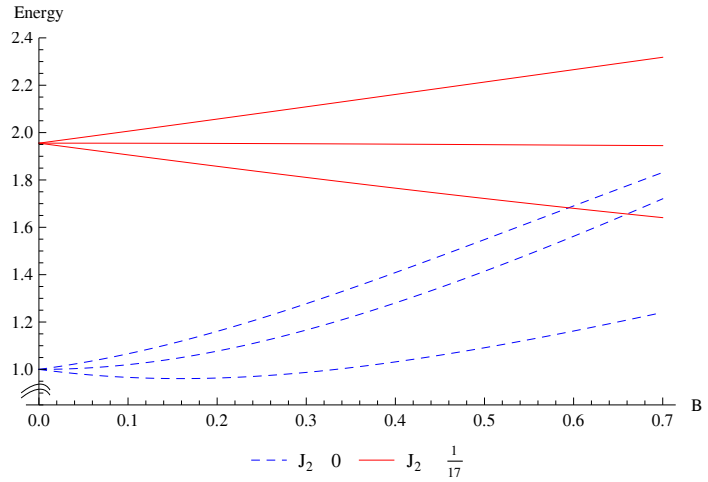

Figure 2.2: Energy of the t_1 triplet excitations versus B in the single site problem (dashed) and as given by RPA at $\mathbf{k} = 0$ (solid). Field and energy are both measured in units of λ.

2.2.3 The Linear B Regime

Computation of the g Factor

In order to characterize the splitting of the magnetic triplet in low field, we can compute an effective g factor in RPA

$$g(\mathbf{k}) = 2 \left. \frac{\partial \epsilon_+(B, \mathbf{k})}{\partial B} \right|_{B=0} \tag{2.23}$$

where we have anticipated that this splitting may depend on wave vector, and included a factor of 2 to account for the fact that $B = 2\mu_B B_{phys}$.[13, 14] Now, if we define the total field felt by the site as

$$B_s = B - \beta^z \tag{2.24}$$

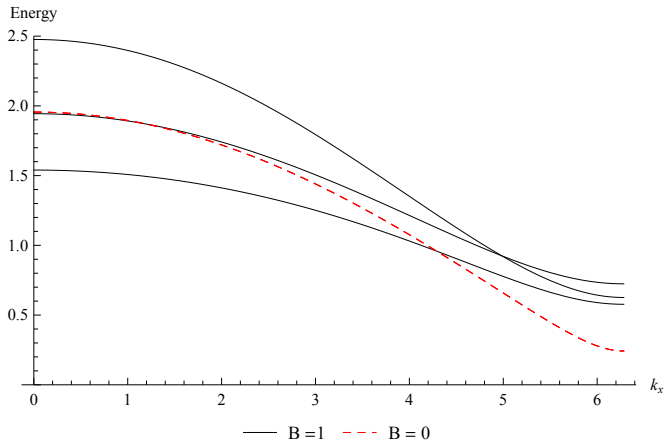

Figure 2.3: Energy of the t_1 triplet excitations versus k_x for a few values of B, at $J_2 = \frac{\lambda}{17}$. Field and energy are both measured in units of λ.

we then find

$$g(\mathbf{k}) = 2 \left.\frac{\partial \epsilon_+(B_s, \mathbf{k})}{\partial B_s}\right|_{B_s=0} \left.\frac{\partial B_s}{\partial B}\right|_{B=0} \tag{2.25}$$

Implicitly differentiating the mean field consistency equation gives

$$\left.\frac{\partial B_s}{\partial B}\right|_{B=0} = \frac{1}{1 + 4\frac{J(\mathbf{0})}{\lambda}} \tag{2.26}$$

For the other derivative, we use first order regular perturbation theory on the polynomial derived from RPA to find

$$2 \left.\frac{\partial \epsilon_+(B_s, \mathbf{k})}{\partial B_s}\right|_{B_s=0} = 1 + 4\frac{J(\mathbf{k})}{\lambda} \tag{2.27}$$

so that

$$g(\mathbf{k}) = \frac{\lambda + 4J(\mathbf{k})}{\lambda + 4J(\mathbf{0})} \tag{2.28}$$

At the zone center, this predicts no modification to the single site g factor of 1. Cu-

riously, we also find that the g factor at the ordering wave vector decreases to zero as we approach the critical point. This agrees well with the qualitative behavior observed in Figure 2.3. Notice also that by $B = 1$ and $J_2/\lambda = 1/17$, we are already well outside of the the linear regime at the ordering wave vector.

Small Fields

In the linear B regime, we actually find that the system responds identically to a static applied field $\mathbf{B} = B\hat{n}$ in *any* direction. To see this, we show that the change in the ground state magnetization and dynamic susceptibility of the single site is isotropic to first order in B. Since these are the only two quantities from the single site problem that enter the calculation of the RPA susceptibility, this is sufficient to show that the response is isotropic at the RPA level. For this section only, B will refer to the magnitude of an arbitrarily directed field, rather than the magnitude of field applied along the (001) direction. So, let $|m\rangle$ denote any exact eigenstate of the single site Hamiltonian in the presence of $\mathbf{B}$ and write

$$|m\rangle = |m_0\rangle + B\,|m_1\rangle + O(B^2) \tag{2.29}$$

For the ground state, we can see

$$|0_1\rangle = \frac{1}{\lambda}\sum_{j\neq 0} |j_0\rangle\,\langle j_0|\hat{n}\cdot\mathbf{S}|0_0\rangle \tag{2.30}$$

giving

$$\mathbf{m} = \frac{\langle 0|\mathbf{S}|0\rangle}{\langle 0|0\rangle^2} = 2B\Re\left[\langle 0_0|\mathbf{S}|0_1\rangle\right] = \frac{4\mathbf{B}}{\lambda} + O(B^2) \tag{2.31}$$

so that the magnetization of the ground state is indeed isotropic to first order in $\mathbf{B}$.

As for the single site susceptibility, we will receive two corrections to first order in B, one from the first order correction to the energies and one from the first order correction to the states. We will write this as

$$\chi_0^{\mu\nu}(\omega, B) = \chi_0^{\mu\nu}(\omega, 0) + B\left(\eta_E^{\mu\nu}(\omega) + \eta_s^{\mu\nu}(\omega)\right) + O(B^2) \tag{2.32}$$

with η_E begin the first order correction from a shift in the energies and η_s being that from the states. Let us focus first on η_s. Investigating the relevant product of matrix elements from the spectral representation for χ_0 gives

$$\begin{aligned}
\langle 0|S^\mu|n\rangle \langle n|S^\nu|0\rangle = &\langle 0_0|S^\mu|n_0\rangle \langle n_0|S^\nu|0_0\rangle \\
&+ B \langle 0_1|S^\mu|n_0\rangle \langle n_0|S^\nu|0_0\rangle \\
&+ B \langle 0_0|S^\mu|n_1\rangle \langle n_0|S^\nu|0_0\rangle \\
&+ B \langle 0_0|S^\mu|n_0\rangle \langle n_1|S^\nu|0_0\rangle \\
&+ B \langle 0_0|S^\mu|n_0\rangle \langle n_0|S^\nu|0_1\rangle + O(B^2)
\end{aligned} \tag{2.33}$$

to first order in B. Since some expectation of the form $\langle n_0|S^\alpha|0_0\rangle$ appears in each of the summands, we can see that this vanishes to first order in B for all states except those that evolve from members of t_1. Furthermore, for $|n_0\rangle \in t_1$, we see that $|n_1\rangle$ is orthogonal to t_1. Since $S^\alpha |0_0\rangle$ lies entirely in t_1, only the first, second and last summands contribute. Using Equation 2.30, we find

$$\eta_s^{\mu\nu} = \frac{4i}{\lambda} \frac{\omega}{\lambda^2 - \omega^2} n_\alpha \epsilon^{\alpha\mu\nu} \tag{2.34}$$

where $\hat{n} = n_\alpha \mathbf{e}_\alpha$ and ϵ is the Levi-Civita symbol. Indeed, this contribution to the dynamic

susceptibility is isotropic.

For η_E, the matrix elements in the spectral representation are all between zeroth order eigenstates, so we can again restrict our attention to the t_1 states. Here we diagonalize the perturbation $(\mathbf{B} \cdot \mathbf{S})$ restricted to t_1 to obtain the zeroth order eigenstates and the first order energies. Only two states receive corrections to their energies at first order. A straightforward computation then produces

$$\eta_E^{\mu\nu} = -\frac{4i\lambda\omega}{(\lambda^2 - \omega^2)^2} n_\alpha \epsilon^{\alpha\mu\nu} \tag{2.35}$$

which we can easily see is also isotropic.

2.3 Response to Electric Fields

2.3.1 Electric Dipole Excitations of a Single Site

Since the tetrahedral symmetry of the single site problem does not include inversion, there is actually a single electric dipole allowed transition from the ground state $a_1 \to t_2$. One would imagine that the story for these excitations ought to be similar to that for the magnetic dipole excitations: the peaks in the permeability due to these excitations will persist in the presence of exchange with a shift in position. In this case, it is actually considerably more difficult to make these statements quantitative for a number of reasons. Perhaps most glaringly in contrast to the question of magnetic dipole excitations, we do not know the identity of the operator which couples the single site problem to an electric field $(\mathbf{P})$. One can demand that such an operator transform as a vector under the point group, i.e. as t_2, but this still leaves the magnitude of its five reduced matrix elements undetermined.

Furthermore, we have no reason to believe that the shift due to the J_2 term ought

to be dominant over those due to all of the other symmetry allowed exchange terms absent in the J_2-λ model. Though J_2 is thought to dominate the other couplings, it only corrects the energy of the electric triplet at second order. Other symmetry allowed terms,[11, 12] e.g. $(T_j^y \mathbf{S}_j) \cdot (T_i^y \mathbf{S}_i)$, give corrections to the energy at first order in their coupling constants that, taken together, might dominate those of J_2. Since there has not yet been an experimentally unambiguous observation of the electric triplet excitation, we abandon the question of quantitatively predicting the shift in its energy.

2.3.2 Collective Response and Critical Behavior

Coupling the Critical Theory to Electric Fields

We can also consider the form of the response to electric field coming entirely from the low-lying magnetic excitations. As we will see, multiple triplon excitations possess the correct symmetry to be produced through coupling to the electric field. To determine the contribution of such processes to the electric field response of our model, we first restrict our considerations to low energy modes near the ordering wave vectors. Either expanding Ω_0 close to the ordering wave vectors and for small frequencies or performing a symmetry analysis[11, 12] produces a Gaussian theory of the form

$$\tilde{S}_{eff}\left[\boldsymbol{\psi}_{a,\mu}\right] = \frac{1}{\beta} \sum_{a,\mu,\omega_n} \int \frac{\mathrm{d}^3\mathbf{k}}{(2\pi)^3} G_\mu^{-1}(\mathbf{k}, i\omega_n) \left|\boldsymbol{\psi}_{a,\mu}(\mathbf{k}, i\omega_n)\right|^2 \tag{2.36}$$

with

$$G_\mu^{-1}(\mathbf{k}, i\omega_n) = -(i\omega_n)^2 + \mathbf{k} V_\mu \mathbf{k} + r^2 = -(i\omega_n)^2 + \epsilon_\mu^2 \tag{2.37}$$

where μ labels which ordering wave vector each of the fields came from, and a labels the sublattice. The matrix V_μ is of the form

$$V_x = \begin{pmatrix} v_1 & 0 & 0 \\ 0 & v_2 & 0 \\ 0 & 0 & v_2 \end{pmatrix} \tag{2.38}$$

with V_y and V_z obtained by permutation. $\boldsymbol{\psi}$ is an order parameter for the staggered magnetization, though depending on how we obtained this theory, $\boldsymbol{\psi}_{a,\mu}$ may not be precisely the staggered magnetization on the a sublattice at the μ ordering wave vector. For one thing, we have rescaled the field in order to set the coefficient of the ω^2 term to 1. Additionally, expectations of Φ are not precisely those of S (c.f. Equation 2.8). We expect that such a theory should describe our system correctly on energy scales small compared to the magnetic bandwidth.

Now, rather than investigate the microscopic origins of the coupling of an electric field to this model, we simply investigate which couplings are allowed by symmetry. We expect couplings through a term linear in the applied field, $E^a P^a$, where P^a is some function of the order parameter. This gives rise to a contribution to the $\mathbf{k} = 0$ electric susceptibility through the standard linear response formalism

$$\chi_e^{ab}(\mathbf{0}, \omega) = \left\langle P^a(\mathbf{0}, \omega) P^b(\mathbf{0}, -\omega) \right\rangle - \left\langle P^a \right\rangle \left\langle P^b \right\rangle \tag{2.39}$$

We do not have couplings before second order in the order parameter, since the order parameter is odd under time reversal while electric fields are even. Beginning at second order without derivatives, we consider what restrictions requiring that a coupling of the

form

$$C^{abc}E^a\psi^b\psi^c \equiv E^a P_0^a \tag{2.40}$$

to transform trivially under the space group places on the tensor C, and hence the polarization P_0^a. We find that the symmetry allowed coupling is given by

$$\begin{aligned} P_0^x =& c_1\left(\psi^y_{A,x}\psi^z_{A,x} - \psi^y_{B,x}\psi^z_{B,x}\right) \\ &+ c_2\left(\psi^y_{A,y}\psi^z_{A,y} - \psi^y_{B,y}\psi^z_{B,y} + \psi^y_{A,z}\psi^z_{A,z} - \psi^y_{B,z}\psi^z_{B,z}\right) \\ &+ c_3\left(\psi^x_{A,y}\psi^y_{B,y} - \psi^x_{B,y}\psi^y_{A,y} + \psi^x_{A,z}\psi^z_{B,z} - \psi^x_{B,z}\psi^z_{A,z}\right) \end{aligned} \tag{2.41}$$

where c_1, c_2 and c_3 are undetermined by this analysis. The other components are related to the x component by simultaneous permutations of the vector and wave vector indicies. Notice that P_0 is odd under interchange of the sublattices, since inversion acts only to interchange the sublattices and gives a sign on the electric field. It can also be shown by expanding the effective action for Φ given in Equation 2.7 that a coupling of the electric field to each site through the single site polarization operator ($\mathbf{P}$) produces a coupling to the critical theory precisely of this form with $c_1 = c_2$ and $c_3 = 0$.

The next lowest order contribution to the electric field response should come from a coupling of the form

$$D^{abcd}E^a\psi^b\partial_c\psi^d \equiv E^a P_1^a \tag{2.42}$$

Due to the larger number of indicies, P_1^x contains many more terms than P_0^x so we omit a detailed discussion of its structure.

Computation of the Electric Susceptibility

Neglecting all couplings of higher order in fields and derivatives, we find the electric susceptibility is given by

$$\chi_e = \chi_{e0} + \chi_{e1} \tag{2.43}$$

$$\chi_{e0}^{ab} = \left\langle P_0^a(\mathbf{0},\omega) P_0^b(\mathbf{0},-\omega) \right\rangle \tag{2.44}$$

$$\chi_{e1}^{ab} = \left\langle P_1^a(\mathbf{0},\omega) P_1^b(\mathbf{0},-\omega) \right\rangle - \left\langle P_1^a \right\rangle \left\langle P_1^b \right\rangle \tag{2.45}$$

since $\langle P_0 \rangle = 0$ and

$$\left\langle P_0^a(\mathbf{0},\omega) P_1^b(\mathbf{0},-\omega) \right\rangle = 0 \tag{2.46}$$

since the internal momentum sum is odd under $\mathbf{q} \to -\mathbf{q}$ while the Green's function is even. Exploiting the particular form of P_0, we find that χ_{e0} is a multiple of the identity and

$$\chi_{e0}^{xx}(\mathbf{0}, i\omega_n) = \frac{\alpha}{\beta} \sum_{\nu_n} \int \frac{\mathrm{d}\mathbf{q}}{(2\pi)^3} G_x(\mathbf{q}, i\omega_n + i\nu_n) G_x(-\mathbf{q}, -i\nu_n) \tag{2.47}$$

with $\alpha = 2c_1^2 + 4c_2^2 + 4c_3^2$. Performing the Matsubara sum and analytically continuing to real frequencies gives

$$\chi_{e0}^{xx}(\mathbf{0},\omega) = \lim_{\delta \to 0^+} \frac{\alpha}{N} \int \frac{\mathrm{d}\mathbf{q}}{(2\pi)^3} \frac{\coth\left(\frac{\beta\epsilon_x(\mathbf{q})}{2}\right)}{\epsilon_x(\mathbf{q}) \left(4\epsilon_x(\mathbf{q})^2 - (\omega + i\delta)^2\right)} \tag{2.48}$$

Allowing $\delta \to 0$ produces

$$\mathrm{Im}\left(\chi^{xx}_{e0}(\mathbf{0},\omega)\right) \propto \mathrm{sgn}(\omega) \int \frac{\mathrm{d}^3\mathbf{q}}{(2\pi)^3} \frac{\coth\left(\frac{\beta\epsilon_x(\mathbf{q})}{2}\right)}{\epsilon_x(\mathbf{q})^2} \delta(|\omega| - 2\epsilon_x) \tag{2.49}$$

$$\propto \Theta(|\omega| - 2\sqrt{r}) \coth(\beta\omega/4) \tag{2.50}$$

Now, as for χ_{e1}, we can see on general grounds that

$$\chi^{ab}_{e1}(\mathbf{0}, i\omega_n) = \frac{\eta^{abcd}}{\beta} \sum_{\nu_n} \int \frac{\mathrm{d}\mathbf{q}}{(2\pi)^3} q_c^2 G_d(\mathbf{q}, i\omega_n + i\nu_n) G_d(-\mathbf{q}, -i\nu_n) \tag{2.51}$$

for some fantastically complicated tensor η. Terms with momentum dependence of the form $q_c q_d$ for $c \neq d$ vanish due to the momentum integration, together with the $\mathbf{q} \to -\mathbf{q}$ symmetry of the Green's function. The restriction that both Green's functions come from the same ordering wave vector comes from demanding that P_1 be invariant under the primitive lattice translations, together with the subtraction of $\langle P_1 \rangle$. On identical grounds to Equation 2.49, we then see

$$\mathrm{Im}\left(\chi_{e1}(\mathbf{0},\omega)\right) \propto \mathrm{sgn}(\omega) \int \frac{\mathrm{d}^3\mathbf{q}}{(2\pi)^3} \frac{q_a^2 \coth\left(\frac{\beta\epsilon_b(\mathbf{q})}{2}\right)}{\epsilon_b(\mathbf{q})^2} \delta(|\omega| - 2\epsilon_b) \tag{2.52}$$

$$\propto \Theta(|\omega| - 2\sqrt{r})(\omega^2 - 4r) \coth(\beta\omega/4) \tag{2.53}$$

2.4 Discussion

2.4.1 Observations of the $a_1 \to t_1$ Excitation

Existing Observations

Two recent THz spectroscopy experiments[4, 5] on $FeSc_2S_4$ have observed a well defined peak at in the range of 4.3meV to 4.5meV, in broad agreement with the previously

estimated magnitude of λ and Equation 2.14.[11, 12] Laurita et al.[5] also performed this experiment in field and extracted results in remarkable agreement with the calculations performed here. To briefly recapitulate their story, they were capable of measuring the dynamic susceptibility in the presence of a field with incident light polarized with magnetic field polarized both along the static applied field direction and transverse to it. At zero field, they observed a peak at ≈ 4.5meV in both polarization configurations. As field increased, the peak in the transverse direction split into two peaks in an approximately linear manner while the peak in the longitudinal direction remained unaffected. Fitting a line to the splitting of the peaks in the transverse susceptibility gave them $g \approx 0.92$.

Following the discussion for Section 2.2.2, this is precisely what we would expect for the case of the field along the (001) direction. We saw that the longitudinal susceptibility (i.e. χ^{zz}) received contributions from only one state and, expanding Equation 2.22 to first order in B, the energy of this state is independent of applied field to first order. The transverse susceptibility (i.e. the x-y block) received contributions from two states of the lower triplet, whose energies split with a g factor just below the single site value of $g = 1$, due to the small wavevector of the incoming light. A priori, we might be surprised that the analysis with B along the (001) direction fits so well to data taken on a polycrystaline sample, but the results of Section 2.2.3 tell us that this is exactly what we should expect, provided we are within the linear regime with respect to the static applied field.

We would be remiss if we did not take this time to say a few words about the nature of the t_1 excitations and what selection rules are relevant to this situation. It is tempting to draw an analogy between the states of t_1 and those of a spin one triplet. Indeed, this analogy motivated the character of the analysis in Section 2.2.2. After all, if we restrict $O(3)$ to T_d, the spin one representation becomes the t_1 representation. So, at least formally, we can label the members of the triplet by $m = 0$ and $m = \pm 1$. In limited ways, this is even reflected in the response to applied field: the $m = 0$ and $m = \pm 1$

states are the zeroth order eigenenstates with respect to the perturbation BS^z and the first order corrections to the energies are 0 and $\pm B/2$, respectively. This is about where the analogy ends, however. The first order corrections to the eigenstates are non-zero (in sharp contrast with a true spin triplet) and there are higher order corrections to the energies of all members of the t_1 triplet.

Furthermore, one might be tempted to attempt to extrapolate selection rules from this analogy, saying that $a_1 \rightarrow t_1$ is spin forbidden as a singlet to triplet transition. This would be incorrect, since in terms of the physical spins the transition is between different states of the $S = 2$ manifold, and no total spin change actually occurs. Since the electronic states see a reduced symmetry due to the crystal field and this reduced symmetry is communicated to the spins through spin orbit coupling, neither total spin nor total orbital angular momentum nor total angular momentum are good quantum numbers on energy scales comparable to λ, and we should not analyze selection rules in terms of them. The proper way to determine the selection rules for transitions between the eigenstates of $\mathcal{H}_i^0$ is through using the Wigner-Eckart Theorem applied to T_d.

Proposal for Future Measurements

The authors are quite taken with the results of the computation of the g factor (Equation 2.28), and hope that it can be successfully measured soon away from $\mathbf{k} = \mathbf{0}$. This would probably require an inelastic neutron scattering measurement on a single crystal. The benefits of such a measurement would be twofold. First of all, the result is unusual and interesting in itself and it would be valuable to see it confirmed in the material. A successful fit of the g factor to the derived form would argue quite strongly for the predictive power of the J_2-λ model for this compound. Secondly, and perhaps more importantly, a fit of the g factor to Equation 2.28 would provide a measurement of the ratio J_2/λ, allowing one to estimate the proximity to the critical point directly.

2.4.2 Continuum Weight in THz Absorption

In addition to their observation of a transition matching the description of the $a_1 \to t_1$ excitation, Mittelstädt et al.[4] observed a curious continuum weight at low frequencies in the dielectric loss which was roughly linear at $T = 80$K and superlinear at $T = 5$K. One can attempt to explain this weight in terms of triplon pair production using the analysis in Section 2.3.2, focusing on the $\omega^2 \coth(\beta\omega/4)$ term that appears in Equation 2.53. At high temperature, $\coth(\beta\omega/4) \approx 4k_BT/\omega$ and we obtain the linear weight. At low temperature, the coth saturates and we obtain weight that grows as ω^2. Within this picture, the fact that this continuum appears at low frequencies then becomes yet another signal of our proximity to the critical point, since we expect this weight only at frequencies in excess of twice the gap to triplon production at the ordering wave vector, as evidenced by the Heavyside Θ in Equation 2.53.

To be fair, there are a few objections that can be raised to this analysis. One could object that without a temperature dependent prefactor the $\omega^2 \coth(\beta\omega/4)$ term fails to reproduce the observed temperature dependence of the absorption. The coth term decreases with increasing temperature, while the lowest frequency weight observed by Mittelstädt et al. increases with increasing temperature. The authors do not find this objection particularly compelling, as one would almost certainly find a temperature dependent prefactor upon a more careful analysis of the temperature dependence. Indeed, if one were to use a finite temperature version of the action in Equation 2.7 and expand about the ordering wave vector for small frequencies, one would find that the velocities in the Green's function in Equation 2.37 depend on temperature. Repeating our analysis that led to Equation 2.53 but keeping more careful track of constants shows that the velocities appear among the (ω) constant prefactor that we have neglected. This is of course to say nothing of possible temperature dependence of the undetermined constants

in the coupling described in Equation 2.42.

Somewhat more concerning is the presence of the two $(const) \times \coth(\beta\omega/4)$ terms appearing in Equations 2.50 and 2.53, which do not reproduce the observed ω dependence. The term in Equation 2.53 can be argued away consistently by claiming that the gap $(\sqrt{r})$ is very small and we do not expect this term to be easily distinguishable in the presence of the large, dominating ω^2. The contribution from Equation 2.50 cannot, to our knowledge, be so concretely claimed as negligible. One might hope that the presence of small but non-zero J_1 might suppress this term by controlling the relative orientations on the A and B sublattices and leading to some cancelation, but this turns out not to be the case. At the Gaussian level, J_1 only acts to slightly reorganize our order parameters, shift the gap slightly and move the soft mode slightly away from the ordering wave vector. Pushing through the calculation, one finds only a change to the gap in Equation 2.50. It seems our only recourse is to argue that the coupling constants (c_1, c_2 and c_3) ought to be small. While this is plausible, the microoscopics of this coupling are quite daunting so we do not present a detailed analysis.

Chapter 3

Instabilities of the Sachdev-Ye-Kitaev and Related Models

3.1 Introduction

The Sachdev-Ye-Kitaev model, a model of N Majorana fermions subject only to quenched disordered interactions, has been an object of considerable study recently, due in part to its rich phenomenology.[16, 17, 18, 19, 20] At finite temperature, the model is amenable to both diagrammatic and replica approaches, with the large N limit reducing to a tractable integral equation which exposes an emergent (approximate) conformal symmetry. This combination of properties sparked considerable interest in the model as a means to study its holographic dual.

Beyond questions of holography, this model also exhibits many properties deserving of study in their own right. To name a few, the disorder-averaged fermion two-point function is gapless and has no poles, prompting an identification of the average model

as a strange metal without quasiparticles. Instabilities of this metal have also been studied as part of the general program to study exotic phases of quantum matter.[20] As $T \to 0$, the entropy density approaches a constant. Finally, despite the Hamiltonians of individual disorder realizations being composed purely of interactions, the replica-saddle point approach exposes that, at leading order in N, the disorder averaged fermion correlation functions obey Wick's theorem indicating that the average model is in some sense free at leading order.

Building on this interest, we attempt in the present work to extend considerations beyond the average model to questions about the full SYK ensemble through some modest studies of questions involving distributions and higher disorder moments of various observables. We also attempt to probe the $T = 0$ physics of this model and further elaborate on studies of its instabilities. Indeed, the $T \to 0$ entropy density seen around the replica diagonal saddle point is itself evidence that the $N \to \infty$ and $T \to 0$ limits cannot be interchanged, since the entropy at $T = 0$ is exactly 0 for any finite N. (Technically speaking, the model could also have an extensive ground state degeneracy, but there is no evidence for this in existing exact digitalization studies.[18]) This indicates a non-analyticity in the $N \to \infty$ limit of the free energy, i.e. a phase transition.

Motivated by the observation that the average fermion correlators obey Wick's theorem and our desire to ask questions about the full distribution, we approach the problem through the variational principle applied to each individual disorder realization, taking as our mean field Hamiltonian a generic free Majorana Hamiltonian. We will see some evidence that the $T = 0$ phase of the SYK model may also break time reversal symmetry, like the ordered phase observed by Bi et al. Finally, we will investigate the disorder statistics of these ordered phases, finding evidence of glassy behavior. While we advance an argument that the ordered phase observed by Bi et al is the same phase as Gaussian random Majorana fermions, we find some evidence that the $T = 0$ phase of the

SYK model is distinct in its disorder statistics and unlikely to be well described by our variational states.

3.2 Formalism and Analytic Results

3.2.1 Setup

We take as our object of study the generalization of the Sachdev-Ye-Kitaev model studied by Bi et al[20], a model of N randomly interacting Majorana fermions η_i with Hamiltonian

$$H = H_0 + uH_u \tag{3.1}$$

$$H_0 = \frac{1}{4!}\sum_{ijkl}^{N} J_{ijkl}\eta_i\eta_j\eta_k\eta_l \tag{3.2}$$

$$H_u = \frac{1}{8}\sum_{ijkl}^{N} B_{ij}B_{kl}\eta_i\eta_j\eta_k\eta_l \tag{3.3}$$

with the entries of J_{ijkl} and B_{ij} totally antisymmetric and drawn from independent, identically distributed gaussians with zero mean and

$$\overline{J_{ijkl}^2} = \frac{J^2}{N^3} \qquad\qquad \overline{B_{ij}^2} = \frac{J}{N^2} \tag{3.4}$$

where $\overline{Q}$ is our notation for the disorder average of the quantity Q. We also define, for our future convenience

$$k = \frac{N}{2} \qquad\qquad M = \frac{N!}{2!(N-2)!} \tag{3.5}$$

As presaged in the introduction, our approach is approximation of the thermal density matrix of each disorder realization by the thermal density matrix of a free Majorana Hamiltonian. To whit, we consider the Gibbs-Delbruck variational principle which states that if

$$\mathcal{F} = -T \ln \mathrm{Tr} \left[\exp \left(-\beta H \right) \right] \tag{3.6}$$

for any trial density matrix ρ_t

$$\mathcal{F} \leq \mathrm{Tr} \left[H \rho_t \right] + T \, \mathrm{Tr} \left[\rho_t \ln \rho_t \right] \equiv \mathcal{F}_t \tag{3.7}$$

This suggests a standard variational approach: we minimize over some tractable class of ρ_t to get the best tractable approximation to $\mathcal{F}$. Notably, this also gives an approximation to the thermal density matrix of a particular disorder realization

$$\rho = \exp \left(-\beta (H - \mathcal{F}) \right) \tag{3.8}$$

since in terms of this quantity the variational principle reads

$$0 \leq \mathrm{Tr} \left[\rho_t \left(\ln \rho - \ln \rho_t \right) \right] \tag{3.9}$$

and we can recognize the quantity on the right as the relative entropy, an information theoretic measure of the difference between two density matrices. Thus the optimum ρ_t for the purposes of approximating the free energy is the closest to the true thermal density matrix in the sense of relative entropy.

We choose as our class of trial density matrices

$$H_t = \frac{i}{2}\sum_{ij}^{N} G_{ij}\eta_i\eta_j \tag{3.10}$$

$$\mathcal{G} = -T \ln \mathrm{Tr}\left[\exp\left(-\beta H_t\right)\right] \tag{3.11}$$

$$\rho_t = \exp\left(-\beta(H_t - \mathcal{G})\right) \tag{3.12}$$

where G, our variational parameter, is any antisymmetric real matrix. Utilizing these trial density matrices should be thought of as doing mean field theory in the observable $\langle\eta_i\eta_j\rangle$. Indeed, one can see that the equations we eventually derive for the optimum G can be identified with the saddle point equations for the field generated in a Hubbard-Stratonovich decoupling of the 4-fermion interaction.

We note for the sake of the fastidious reader that when we refer to "Gaussian random free Majoranas" we mean an ensemble of Hamiltonians of the form given in Equation 3.10 with G_{ij} drawn from independent, identically distributed Gaussians with zero mean and

$$\overline{G_{ij}^2} = \frac{J}{N} \tag{3.13}$$

Though we will find later that the parametrization of this class of density matrices by G is profitable in a numerical context, we make a change of variables in order to explore the broad character of the minima. There is some $\Phi \in O(N)$ such that defining

$$\xi_i = \sum_j \Phi_{ij}\eta_j \tag{3.14}$$

give new cannonical Majoranas ξ_i in terms of which we have

$$H_t = \frac{i}{2}\sum_{\mu}^{k} g_\mu \xi_{2\mu-1}\xi_{2\mu} \tag{3.15}$$

where the spectrum of G is $\pm i g_\mu$ and we have chosen $g_\mu \geq 0$. We will refer to this Φ as "diagonalizing" G, since

$$\Phi^t G \Phi = \sum_{\mu}^{k} g_\mu e^\mu \tag{3.16}$$

where

$$e^{ij}_{kl} = \delta_{i,k}\delta_{j,l} - \delta_{i,l}\delta_{j,k} \tag{3.17}$$

$$e^\mu = e^{2\mu-1,2\mu} \tag{3.18}$$

Equation 3.15 implies

$$\langle \xi_{2\mu-1}\xi_{2\mu}\rangle_t = -i\tanh\left(\frac{g_\mu}{T}\right) \equiv -id_\mu \tag{3.19}$$

where

$$\langle A\rangle_t = \mathrm{Tr}\left[A\rho_t\right] \tag{3.20}$$

Reversing the transformation, we find

$$\langle \eta_i\eta_j\rangle_t = \frac{\delta_{ij}}{2} - iC_{ij} \tag{3.21}$$

with

$$iC = \tanh\left(\frac{iG}{T}\right) \tag{3.22}$$

where for any holomorphic function $f(z)$ and Hermitian matrix X we have defined

$$f(X) = \frac{1}{2\pi i}\oint_\gamma f(z)\,(z\mathbb{I} - X)^{-1}\,\mathrm{d}z \tag{3.23}$$

where γ is some contour enclosing the spectrum of X and $\mathbb{I}$ is the identity matrix.

For any $T > 0$, $C(G,T)$ is a diffeomorphism from all antisymmetric real matrices to antisymmetric real matrices with eigenvales with absolute value strictly less than 1. Since it is a diffeomorphism, we may consider our trial free energy (and density matrices) to be a function of C rather than G. For future use, we define $\mathcal{A} \cong \mathbb{R}^M$ to be the space of all antisymmetric real matrices, $\mathcal{C} \subset \mathcal{A}$ to be those matrices with eigenvalues with absolute value strictly less than 1 and $\overline{\mathcal{C}} \subset \mathcal{A}$ to be those matrices with eigenvalues with absolute value less than or equal to 1.

Thinking of C as our variational parameter also allows us to slightly expand our class of variational density matrices in a critical way. For any $C \in \mathcal{C}$, we can write

$$C = \Phi\left(\sum_\mu^k d_\mu e^\mu\right)\Phi^t \tag{3.24}$$

Diagonalizing H_t, we can find that this C maps to the density matrix

$$\rho_t(C) = 2^{-k}\sum_{s\in\mathbb{Z}_2^k}\left(\prod_\mu^k(1 + s_\mu d_\mu)\right)|\Phi, s\rangle\langle\Phi, s| \tag{3.25}$$

where $|\Phi, s\rangle$ is the ground state of the free fermion Hamiltonian

$$\frac{i}{2}\sum_{ij}\tilde{G}_{ij}\eta_i\eta_j \qquad\qquad \tilde{G} = \Phi\left(\sum_{\mu} s_\mu e^\mu\right)\Phi^t \tag{3.26}$$

and we have identified $\mathbb{Z}_2$ with $(\{\pm 1\}, \cdot)$. This formula can manifestly be extended to give a well defined density matrix for any $C \in \overline{\mathcal{C}}$. Since $\overline{\mathcal{C}}$ is compact, this guarantees that the trial free energy will attain a minimum on this class of density matrices.

This extension is not merely a curiosity, but necessary to obtain a minimum at $T = 0$. This is to be expected, since $\partial\mathcal{C} = \overline{\mathcal{C}} - \mathcal{C}$ corresponds to density matrices of less than full rank: in particular it contains the pure states corresponding to the ground states of free Majorana Hamiltonians.

To put a fine point on it, fix $\Phi \in SO(N)$ arbitrary and consider the zero temperature minimum with respect to d_μ. At $T = 0$, we have

$$\mathcal{F}_t = 2^{-k}\sum_{s\in\mathbb{Z}_2^k}\left(\prod_{\mu}^{k}(1 + s_\mu d_\mu)\right)\langle\Phi, s|H|\Phi, s\rangle \tag{3.27}$$

Some $s_0 \in \mathbb{Z}_2^k$ has the minimum expectation value of the energy $\langle\Phi, s_0|H|\Phi, s_0\rangle$ and clearly $\mathcal{F}_t$ is then minimized with respect to d by choosing $d = s_0$, corresponding to the pure state $|\Phi, s_0\rangle$. So, at $T = 0$, the minimum is always attained on $\partial\mathcal{C}$.

3.2.2 Properties of the minima

In terms of C, a lengthy but straightforward calculation gives

$$\mathcal{F}_t = E - TS \tag{3.28}$$

$$E = \frac{1}{2}\langle C, LC\rangle - \frac{u}{2}\|B\|^2 \tag{3.29}$$

$$L = K + uU \tag{3.30}$$

$$S = N\ln(\sqrt{2}) - \frac{1}{2}\operatorname{Tr}\left[(\mathbb{I} + iC)\ln(\mathbb{I} + iC)\right] \tag{3.31}$$

where we have defined the inner product and norm on $\mathcal{A}$

$$\langle X, Y\rangle = \frac{1}{2}\operatorname{Tr}\left[XY^T\right] \tag{3.32}$$

$$\|X\| = \sqrt{\langle X, X\rangle} \tag{3.33}$$

and J and U are linear functions $\mathcal{A} \to \mathcal{A}$ defined by

$$\langle X, KY\rangle = -\frac{1}{4}\sum_{ijkl}^{N} J_{ijkl}X_{ji}Y_{kl} \tag{3.34}$$

$$\langle X, UY\rangle = -\langle X, B\rangle\langle B, Y\rangle - \langle X, BYB\rangle \tag{3.35}$$

We will write the latter as

$$U = -B \otimes B - B \boxtimes B \tag{3.36}$$

Since it is actually composed of two different tensor products of B. $B \otimes B$ refers to the tensor product of B with itself considered as a vector (in $\mathbb{R}^M$, c.f. the operator $|\alpha\rangle\langle\alpha|$) while $B \boxtimes B$ is the tensor product of B with itself considered as an operator on $\mathbb{R}^N$

projected onto the subspace of antisymmetric matrices ($\Lambda^2(\mathbb{R}^N)$).

Now, in order to characterize the minimum of the free energy as a function of C, we must take derivatives of $\mathcal{F}_t$ with respect to C. This computation is lengthy and not particularly informative, so we relegate it to Appendix A.1. There, we find

$$\nabla_C \mathcal{F}_t = L(C) + G \tag{3.37}$$

So that our minimum must have

$$L(C) = -G \tag{3.38}$$

We also have for the Hessian (the matrix of second derivatives)

$$\mathrm{Hess}_C(\mathcal{F}_t) = L - T\,\mathrm{Hess}_C(S) \tag{3.39}$$

As for $-\mathrm{Hess}_C(S)$, we give a more thorough characterization in Appendix A.1 and for now simply note that its eigenvalues are given by

$$\frac{g_\mu \pm g_\nu}{d_\mu \pm d_\nu} \text{ and } \frac{1}{1-d_\mu^2} \tag{3.40}$$

Using the concavity of $(1+x)\ln(1+x) + (1-x)\ln(1-x)$ on $(-1,1)$, we can see that the former is bounded below by the latter. The latter is then easily seen to be bounded below by 1, which implies that $-(\mathbb{I}+\mathrm{Hess}_C(S))$ is non-negative. So, if λ_m is the minimum eigenvalue of L, for $T > |\lambda_m|$ $\mathcal{F}_t$ is convex in C. Since $\overline{\mathcal{C}}$ is convex, $\mathcal{F}_t$ must have a unique minimum. Since one can easily see that $\nabla_C \mathcal{F}_t|_{C=0} = 0$ this minimum occurs at $C = 0$, giving $G = 0$ and $\rho_t = \mathbb{I}$.

For $T < |\lambda_m|$, though, the extremum at the origin becomes a saddle point. To whit,

$$\text{Hess}_C(\mathcal{F}_t)|_{C=0} = L + T\mathbb{I} \tag{3.41}$$

so that at $T = \lambda_m$ the minimum eigenvalue of the hessian passes through zero and the minimum moves off of the origin, stabilized by higher order terms in S. For $T < |\lambda_m|$, there are actually a pair of minima away from the origin related by time reversal symmetry. That is, in the language of mean field theory, the individual disorder realization breaks time reversal symmetry ($G \to -G$) at the mean field level. We do not have an argument that these local minima remain the global minima below the transition temperature, and will simply ignore the question in this work.

3.2.3 Order Parameter

We adopt the convention that a quantity Q evaluated at the minimum will be denoted Q_*. $\|C_*\|^2$ is an order parameter for the time reversal symmetry breaking, so it is natural to ask what implication it has for possible glassy order. $\|C_*\|^2$ is in some sense a natural analogue of the Edwards-Anderson order parameter[21], since

$$\|C_*\|^2 = -\sum_{ij} \langle \eta_i \eta_j \rangle_{t*} \langle \eta_i \eta_j \rangle_{t*} \tag{3.42}$$

or, in the language of replicas

$$\overline{\|C_*\|^2} = -\sum_{ij} \left\langle \eta_i^\alpha \eta_j^\alpha \eta_i^\beta \eta_j^\beta \right\rangle \tag{3.43}$$

Thus, the presence of nonzero $\overline{\|C_*\|^2}$ in the thermodynamic limit is our signal that the physics is governed by a non replica-diagonal saddle point (i.e. "spin glass" order) and a

lack of self averaging in $\|C_*\|^2$ is our signal for replica symmetry breaking.[22]

We note in passing that $\overline{\|C_*\|^2}$ contains all non-trivial information from the first two disorder moments of the distribution of $\|C_*\|^2$, due to the $O(N)$ statistical symmetry of the SYK model. It is trivial to see that this symmetry forces $\overline{C_*} = 0$. However, it also gives that

$$\overline{C_{ij*}C_{kl*}} = (\delta_{ik}\delta_{jl} - \delta_{il}\delta_{kj}) \frac{2\overline{\|C_*\|^2}}{N(N-1)} \tag{3.44}$$

by applying Schur's Lemma to the adjoint representation of $SO(N)$. While the fundamental reflections in $O(N)$ allow us to see that the third disorder moment must be zero, the fourth disorder moment is in general allowed to be more complicated. In this work, we study only $\overline{\|C_*\|^4}$ as a test of self-averaging in $\|C_*\|$.

To forestall questions of whether these correlations are sub-leading, we note that

$$0 \leq -\frac{1}{2}\sum_{i\neq j} \langle \eta_i\eta_j\rangle \langle \eta_i\eta_j\rangle \leq \frac{N}{2} \tag{3.45}$$

for any density matrix, not just a thermal density matrix of a free Majorana Hamiltonian. To see this, notice that

$$M_{ij} = \langle \eta_i\eta_j\rangle - \frac{\delta_{ij}}{2} \tag{3.46}$$

is an antisymmetric Hermitian matrix by the properties of the Majorana operators. So there must be $\tilde{\Phi} \in O(N)$ such that

$$M = \tilde{\Phi}\left(\sum_{\mu}^{k} im_\mu e^\mu\right)\tilde{\Phi}^t \tag{3.47}$$

and defining the new cannonical Majoranas

$$\tilde{\xi}_i = \sum_{ij}^{N} \tilde{\Phi}_{ij} \eta_j \tag{3.48}$$

we find

$$|m_\mu| = \left| \left\langle \tilde{\xi}_{2\mu-1} \tilde{\xi}_{2\mu} \right\rangle \right| \leq 1 \tag{3.49}$$

implying

$$-\frac{1}{2} \sum_{i \neq j} \langle \eta_i \eta_j \rangle \langle \eta_i \eta_j \rangle = \sum_{\mu}^{k} m_\mu^2 \leq \frac{N}{2} \tag{3.50}$$

Since the minimum is attained by a pure state at $T = 0$, we have

$$\|C_*\|^2 \big|_{T=0} = \frac{N}{2} \tag{3.51}$$

for every disorder realization. So, this implies that

$$\overline{\|C_*\|^2} \Big|_{T=0} = \frac{N}{2} \tag{3.52}$$

and $\overline{\|C_*\|^2}$ saturates this bound at $T = 0$.

3.2.4 Large N scaling

Beyond this point, making further analytic progress seems daunting, since we must exert some understanding of the random symmetric real matrix L. L is not drawn from any well studied matrix ensemble the authors are aware of, rendering hope of this understanding slim. Some partial progress and modest intuition can be developed about

L's constituent parts, however, which can then be checked numerically.

We begin with U, since the distribution of B is relatively well understood. First, we can notice that $B \otimes B$ is rank one with nonzero eigenvalue

$$\lambda_{\otimes} = \|B\|^2 \tag{3.53}$$

It is a trivial application of the central limit theorem to see that

$$\sqrt{\frac{N(N-1)}{3J^2}} \left(\frac{N^2}{N(N-1)} \lambda_{\otimes} - \frac{J}{2} \right) \xrightarrow{d} N(0,1) \tag{3.54}$$

where $N(\mu, \sigma)$ denotes a normally distributed random variable with mean μ and variance σ^2, so that in the large N limit, $\lambda_{\otimes}$ becomes narrowly distributed around J.

Our understanding of $B \boxtimes B$ is more limited, but some can still be said without straining. Since the eigenvalues of the tensor product of two operators are the product of the eigenvalues of the operators, we find the bound for the operator norm

$$\|B \boxtimes B\|_{op} \leq \|B\|_{op}^2 \tag{3.55}$$

Since iB is drawn from a Hermitian Wigner matrix ensemble, we have[23]

$$\|B\|_{op} = O\left(\frac{1}{\sqrt{N}} \right) \tag{3.56}$$

and so

$$\|B \boxtimes B\|_{op} = O\left(\frac{1}{N} \right) \tag{3.57}$$

Before synthesizing these results, we say what we can about K. Unfortunately, this

amounts entirely to conjecture that will be borne out in our numerical results. K bears some resemblance to a sample from a symmetric Wigner matrix ensemble, except for the fact that

$$\left\langle e^{ij}, Ke^{ik} \right\rangle = 0 \tag{3.58}$$

for every i, j and k. This violates the independence assumption and prevents us from rigorously applying any of those results. Heuristically, however, we can notice that there are $\begin{pmatrix} M \\ 2 \end{pmatrix}$ off diagonal elements and only $\begin{pmatrix} N \\ 3 \end{pmatrix}$ of them are correlated. So, the proportion of them that are correlated is

$$\frac{\begin{pmatrix} N \\ 3 \end{pmatrix}}{\begin{pmatrix} M \\ 2 \end{pmatrix}} = O\left(\frac{1}{N}\right) \tag{3.59}$$

and it is perhaps reasonable to expect that we have

$$\|K\|_{op} = O\left(\frac{1}{\sqrt{N}}\right) \tag{3.60}$$

as we would were K actually drawn from a symmetric Wigner distribution.

As to what this means for our minimization problem, we have the simple eigenvalue bound

$$\lambda_m \geq -\|K\|_{op} - u\|B \boxtimes B\|_{op} - u\Theta(u)\lambda_{\otimes} \tag{3.61}$$

giving

$$\lambda_m = \begin{cases} O(1) & u > 0 \\ O\left(\frac{1}{\sqrt{N}}\right) & u \leq 0 \end{cases} \tag{3.62}$$

provided that our conjecture about the scaling of λ_K is correct.

Assuming that where it is nonzero $\|C_*\|^2 = O(N)$ (as is suggested by Equation 3.51), we can use Equation 3.62 to deduce the scaling of a few other quantities. Notably, we find

$$E_* = \begin{cases} O(N) & u > 0 \\ O(\sqrt{N}) & u \leq 0 \end{cases} \tag{3.63}$$

which casts serious doubt on how well this approximation captures the $T = 0$ physics of the model for $u \leq 0$, since we expect an extensive (i.e. $O(N)$) ground state energy for all u. This question will be discussed in more detail in Section 3.4. Finally, we notice that the minimum condition allows us to see

$$\|G_*\|^2 = \begin{cases} O(N) & u > 0 \\ O(1) & u \leq 0 \end{cases} \tag{3.64}$$

3.2.5 The Susceptibility and Heat Capacity

We also compute an approximation to the susceptibility and heat capacity within this framework. The details of this computation are given in Appendix A.2. There, we find that the susceptibility shows a singularity of the form

$$\chi_0 \sim \frac{\text{sgn}(|\lambda_m| - T)}{|\lambda_m| - T} \tag{3.65}$$

We can compute a crude approximation to the average of the susceptibility by simply integrating this expression against the distribution of the lowest eigenvalue λ_m:

$$\overline{\chi_0} \sim \int_{-\infty}^{\infty} \frac{\mathrm{sgn}(|\lambda_m| - T)}{|\lambda_m| - T} p(\lambda_m) \mathrm{d}\lambda_m \tag{3.66}$$

which, combined with our expectation that $p(\lambda_m)$ should be supported on all of $(0, \infty)$ for finite N, yields an integral that does not exist. That is, we can conclude that the disorder average for this approximation to the susceptibility does not exist at finite N.

Heuristically, one should perhaps think about this result in the reverse direction. At any given temperature, there's a finite probability of finding the transition temperature of a disorder realization within any given small region around the temperature of interest. Given the strength of the singularity in the susceptibility, these nearby transitions have large enough values of the susceptibility to prevent the average from converging at the temperature of interest. It is perhaps illustrative to consider circumstances under which this could fail to happen. If the singularities predicted in an individual disorder realization were less severe, say $|T - |\lambda_m||^{-1/2}$, this integral would converge and our heuristic would predict finite disorder averages. There, we would be saved by the fact that we do not have finite probability of finding the transition *precisely* at the temperature of interest and the nearby transitions are not strongly enough singular to make up for this fact.

We note in passing that this behavior is certainly an artifact of our variational approximation. For finite N, the true free energy is analytic in the probe field defined in Appendix A.2. We should perhaps have expected worse behavior out of the susceptibility than our other quantities of interest, since it is not controlled directly by a variational principle like our other quantities of interest (with the exception of the heat capacity). We also note that its possible that a prediction of the susceptibility in this framework might be salvageable with more careful analysis, since λ_m self-averages at large N which

appears to superficially address the issue. A careful examination of this approach and whether it can be accessed numerically is outside the scope of the present work, however, and we make no further inquiry into the susceptibility.

As for the heat capacity, the expression given in Equation A.37 bears some investigation for any dangerous singularities given our experience with a similar expression for the susceptibility. However, considering a Landau-type expansion in small G near $T = |\lambda_m|$ leaves one with the expectation that

$$\|G_*\| = O\left((|\lambda_m| - T)^{1/2}\right) \tag{3.67}$$

as $T \to |\lambda_m|^-$ so that counting powers of $|\lambda_m| - T$ then suggests that $C_V = O(1)$ in this limit. Numerically, we see no evidence of a singularity in the heat capacity in an individual disorder realization, though note a discontinuity in the heat capacity at $T = |\lambda_m|$.

3.3 Numerical Results

To complement our analysis above, we numerically find the minima of randomly generated samples of L to characterize the statistics of various quantities at the minimum. All of our code was written in Python 2.7.14 using SciPy 1.0.0 and NumPy 1.14.0 and run on the CNSI "Knot" cluster at UCSB. After a sample of L is generated, its minimum eigenvalue and the associated eigenvector are found using SciPy's eigh function. The code then searches for a minimum of $\mathcal{F}_t$ as a function of G using BFGS as implemented in SciPy's minimize function, starting with the temperature just below the minimum eigenvalue and with an initial guess just away from the origin in the direction of the minimum eigenvector of L. After a minimum is found at a given temperature, the code

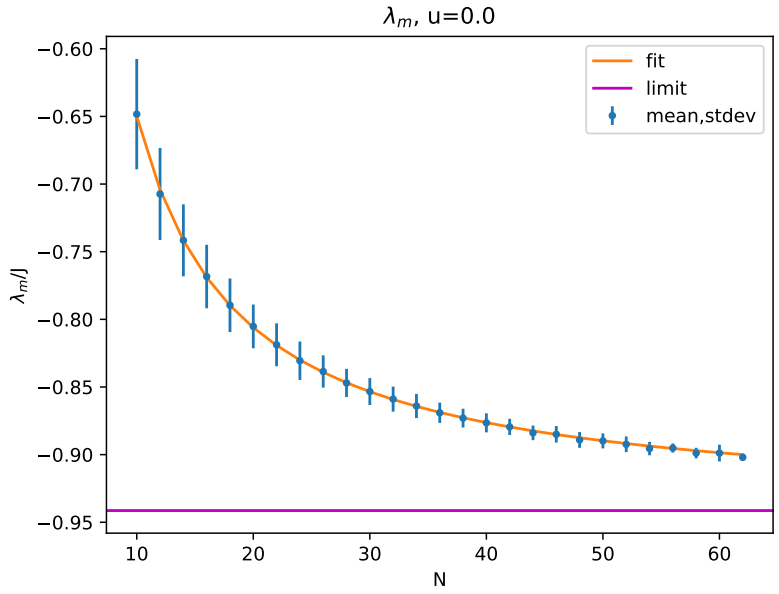

Figure 3.1: Averages and mean squared errors for λ_m for $u = 0$, together with fit line and limiting value.

decreases the temperature by a predetermined step and searches for the minimum starting at the previous minimum. An exact value for the gradient with respect to G is provided, as calculated in Appendix A.1. We choose to minimize with respect to G rather than C to avoid having to numerically enforce the eigenvalue constraint. We of course study the quantities $\mathcal{F}_{t*}$, E_*, S_* and C_V. To track some information about the minimizing state and the resulting distribution, we also track $\|C_*\|^2$ and $\|G_*\|^2$.

To counteract the fact that we expect $\overline{\lambda}_m \to 0$ for $u \leq 0$, we rescale the model and study instead

$$\tilde{L} = \begin{cases} 2L & u > 0 \\ \frac{3\sqrt{N}}{4} L & u \leq 0 \end{cases} \tag{3.68}$$

This rescales all quantities with dimensions of energy identically, so $\tilde{T}$ and $\tilde{G}$ are rescaled by the same factors. The factors of two exist to move the limiting value of $\overline{\lambda}_m$ close to J

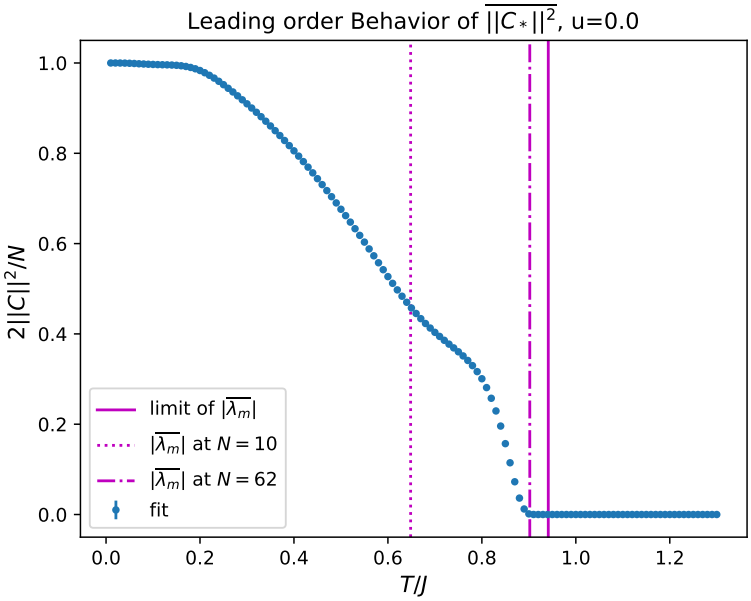

Figure 3.2: Coefficient of N in $\|C_*\|^2$ regression for $u = 0$, with error bars.

as observed empirically. All N dependencies given in this section will be given in terms of the rescaled model, rather than the original model. Because of our limited computational resources, we study only three values of u, $u = \pm 1$ and $u = 0$. These values were chosen with the expectation from Bi et al's work and our analysis so far that there are only two relevant regions of u, $u \leq 0$ and $u > 0$ together with a modest degree of hedging that the $u = 0$ case might conceivably be special.

We are interested in the leading order large N behavior of our quantities of interest as a function of temperature. However, only $N \leq 62$ is numerically accessible to us without considerable effort. Our numerical efforts produced 500 samples for $N = 10$ through $N = 30$ and a steadily decreasing number of samples through $N = 62$ where we received only 12 samples. We sampled every available N in this range, i.e. every even N. Consequently, we must work just a little bit to extract information about the large N limit with our available data. Our analysis largely follows White[24] with some trivial modifications, but we present the techniques here to ensure we are clear about what we

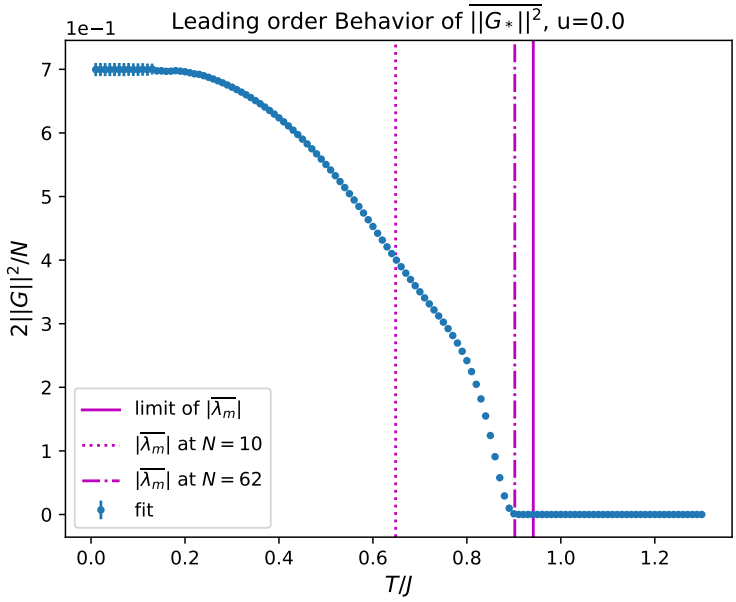

Figure 3.3: Coefficient of N in $\|G_*\|^2$ regression for $u = 0$, with error bars.

mean by each quantity and in case the reader is unfamiliar. We will be concerned with two questions for all of our quantities of interest: what is the leading order behavior of their average and do they exhibit self-averaging.

For the first question, consider some quantity $y = O(N^\nu)$. Largely we will be concerned with quantities with $\nu = 1$, with the exception of λ_m which has $\nu = 0$. We will attempt to fit our observations to a model of the form

$$y_i = \sum_{j=0}^{2} N_i^{\nu-j} y_{f,j} + \epsilon_i \tag{3.69}$$

where i stands for the ith of n independent observations at various N and $\epsilon_i = y_i - \overline{y}_i$. As is standard for regression problems, we phrase this in terms of matrices as

$$Y = \mathcal{N} Y_f + \epsilon \tag{3.70}$$

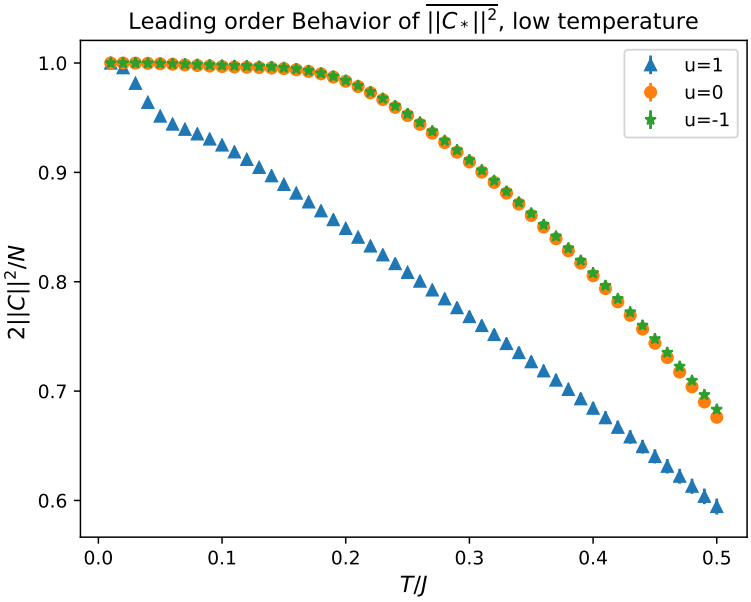

Figure 3.4: Coefficient of N in $\|C_*\|^2$ for various u at low temperature.

where Y is now a $n \times 1$ vector of observations, $\mathcal{N}$ is our $n \times 3$ "design matrix" which contains the powers of N we expect the averages to depend on and Y_f is a 3×1 vector of our unknown fit parameters.

The critical difference between this situation and a standard regression problem is that the variances of the ϵ_i are both unknown and expected not to be equal. Even so, if we define the ordinary least squares estimator

$$\hat{Y}_f = \left(\mathcal{N}^t \mathcal{N}\right)^{-1} \mathcal{N}^t Y \tag{3.71}$$

and the variance estimator

$$\hat{V} = \left(\mathcal{N}^t \mathcal{N}\right)^{-1} \mathcal{N}^t \hat{R} \mathcal{N} \left(\mathcal{N}^t \mathcal{N}\right)^{-1} \tag{3.72}$$

$$\hat{R}_{ij} = \delta_{ij} \left(y_i - \left[\mathcal{N} \hat{Y}_f\right]_i\right)^2 \tag{3.73}$$

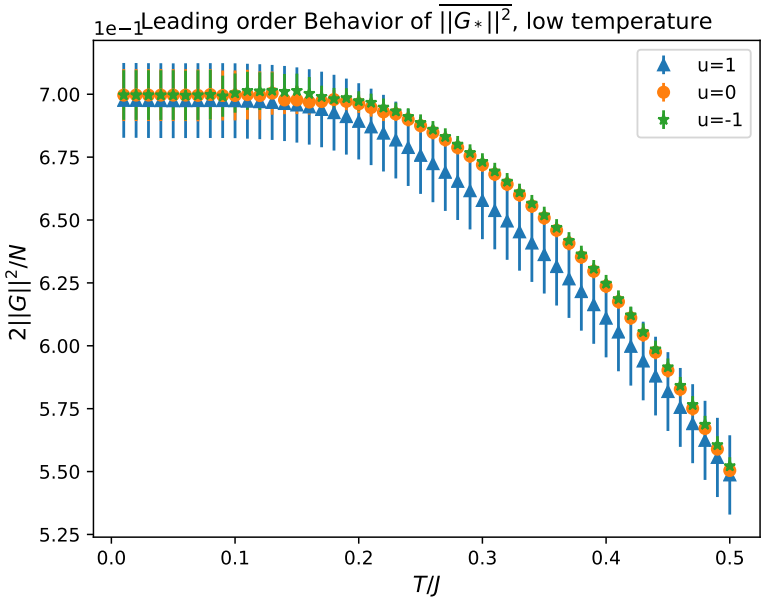

Figure 3.5: Coefficient of N in $\|G_*\|^2$ for various u at low temperature.

White[24] shows that as the number of observations grows

$$\hat{V}^{-1/2}\left(\hat{Y}_f - Y_f\right) \xrightarrow{d} N(0, \mathbb{I}_3) \tag{3.74}$$

Since one can observe that $\hat{V} = O(n^{-1})$, where n is the number of observations, this shows that $\hat{Y}_f$ is still a consistent estimator for our fit parameters. This also allows us to compute confidence intervals for these parameters (albeit only asymptotically correct ones). All confidence intervals quoted will be the 99% confidence windows under the asymptotic distribution.

The question of self-averaging requires a modicum more work, since we must be careful about what exactly constitutes an observation of the variance. One could imagine a number of ways to organize this information, but we simply use all data points taken at a particular N to construct an estimate of the variance at that N and count this as a single observation of the variance. Since y undergoes self averaging if $y^2 - \overline{y}^2 = O(N^{2\nu-1})$

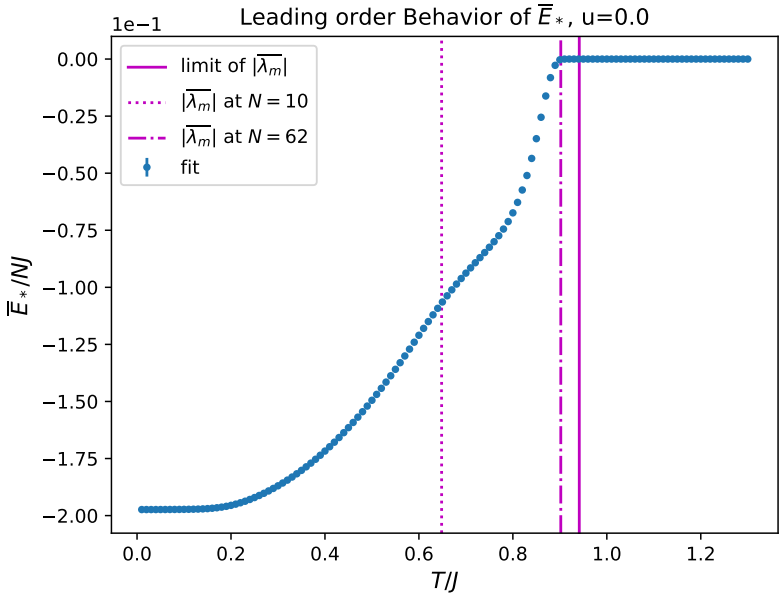

Figure 3.6: Coefficient of N in E_* regression for $u = 0$, with error bars.

rather than $O(N^{2\nu})$, we probe self-averaging by fitting our observed values of the variance to $N^{2\nu}$ through $N^{2\nu-3}$ and reporting the leading order coefficient with 99% confidence windows.

By this point, there is relatively little in the numerical results that is a surprise, since we have already conjectured all of our highest leverage results. The scalings conjectured in Section 3.2.4 are consistent with our observed scalings in the rescaled model. Comfortingly, we find that the fit to the data for λ_m gives for $u = 1$ that $\lambda_m \to 0.99 \pm 0.01$, which is consistent with the limiting value one would expect from assuming $\lambda_\otimes$ is the dominant contribution to the large N limit and using Equation 3.54. In particular, our results strongly argue that our scaling expectations for $\|C_*\|^2$ (FIG. 3.2) are correct, an indication of glassy behavior in the model. We also note the consistency of the numerical results of these quantities with many of their known $T = 0$ limiting values.

Looking at our results as a whole, two broad trends bear discussion first. The first of these themes is that the results for $u = -1$ and $u = 0$ look nigh identical to the

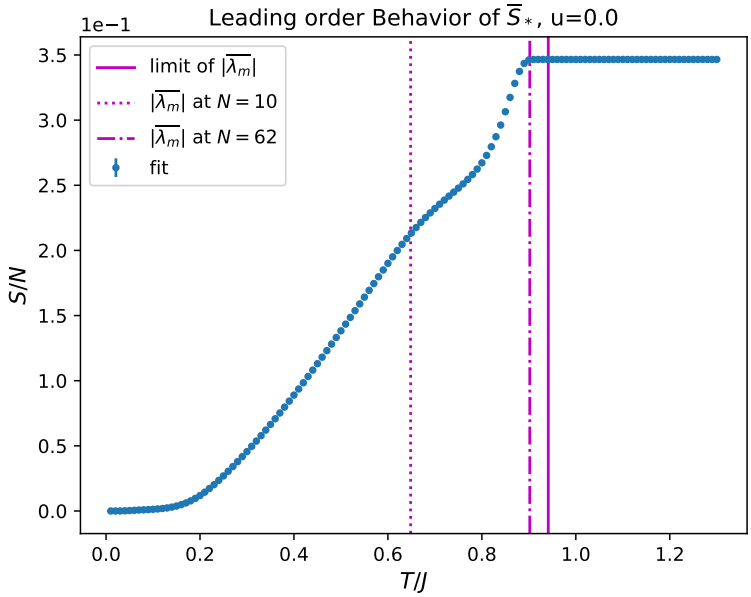

Figure 3.7: Coefficient of N in S_* regression for $u = 0$, with error bars.

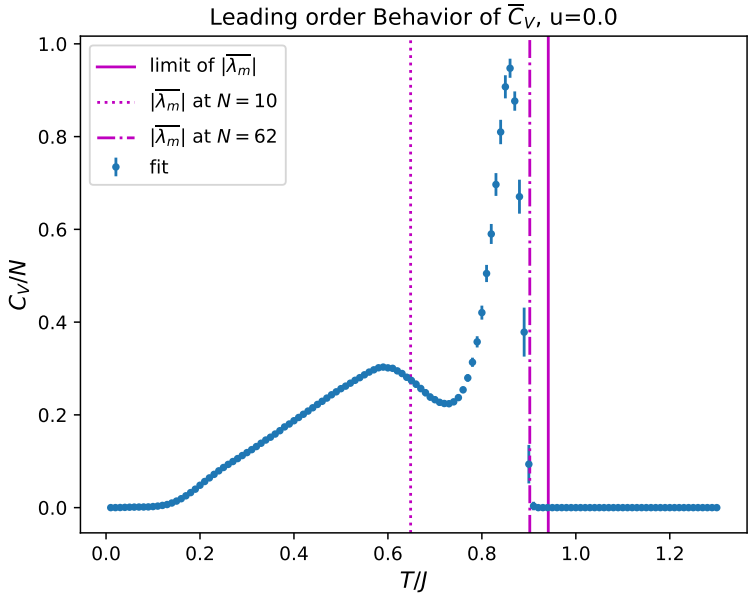

Figure 3.8: Coefficient of N in C_V regression for $u = 0$, with error bars.

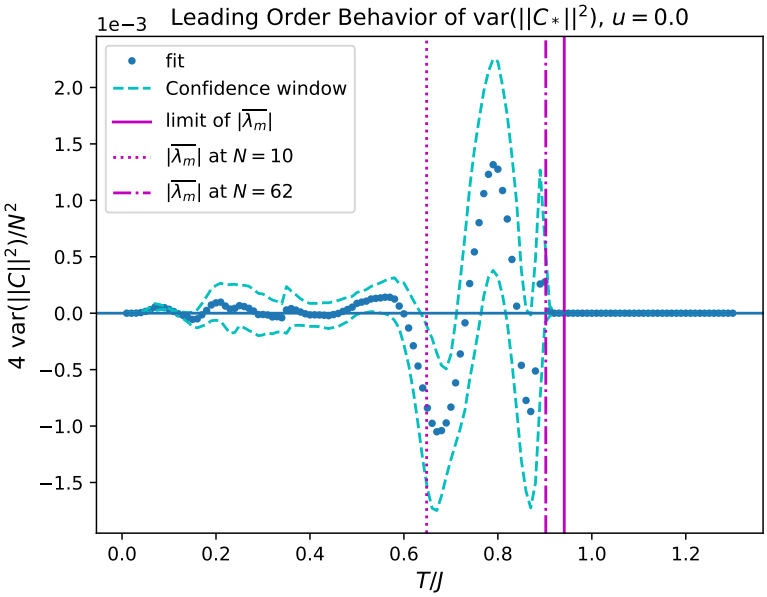

Figure 3.9: Coefficient of N^2 in of $\|C_*\|^2$ regression for $u = 0$, with confidence window.

human eye. One might have expected this given the information on $B \boxtimes B$ presented in Section 3.2.4, since this term is expected to be sub-leading relative to K. One might also have expected this on the basis that previous study of this model indicates $u \leq 0$ should all be a single phase.[20] A close inspection of the data for $\|C_*\|$ at $u = 1$, however, reveals a subtle feature at low temperature (FIG. 3.4) that is hard to conclusively make sense of with the available data. The authors conjecture that this is due to differences in the angular distribution (or eigenvalue distribution, if the reader prefers) of G_*, about which more will be said in Section 3.4. This conjecture is supported by the presence of this feature in our data for S_* and C_V along with the lack of any such feature in the data for $\|G_*\|^2$ and is consistent with the lack of this feature in the data for E_* and $\mathcal{F}_{t*}$.

On the second theme: we note a few regions in the plots which almost certainly show finite size effects. The most clear instance of this is the lack of an $O(N)$ component in the temperature range between the limiting value of $\left|\overline{\lambda_m}\right|$ and the value of $\left|\overline{\lambda_m}\right|$ at our final N point, $N = 62$. We have a strong expectation that this region of temperatures

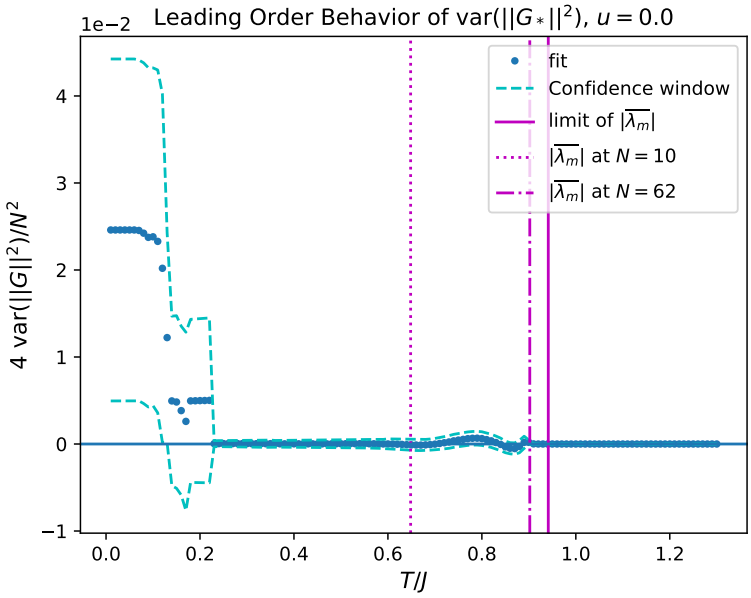

Figure 3.10: Coefficient of N^2 in of $\|G_*\|^2$ regression for $u = 0$, with confidence window.

should actually be in the ordered phase, but samples of disorder realizations with $|\lambda_m|$ greater than the average value at $N = 62$ are quite rare at all of the N points that we sample. This is perhaps more intuitive upon looking at our fits of the observed λ_m (FIG. 3.1) where one can notice that λ_m appears to self average more rapidly than it converges to its limiting value. This accounting is supported by the fact that the plots for $u = 1$ show this feature much less strongly while λ_m appears to self average much more slowly for $u = 1$. For similar reasons, we regard any dramatic features in the fits in the region between the values of $\left|\overline{\lambda_m}\right|$ for $N = 10$ and $N = 62$ with a mild suspicion, as temperatures further to the right of that region spend progressively more of our sample artificially above the transition temperature.

One might reasonably rouse some suspicion towards our statistical analysis on these grounds, since it does not raise any red flags in the form of wider confidence intervals in most of our quantities in these regions. However, ultimately this is not so surprising since these finite size effects represent "unknown unknowns" from the point of view of the

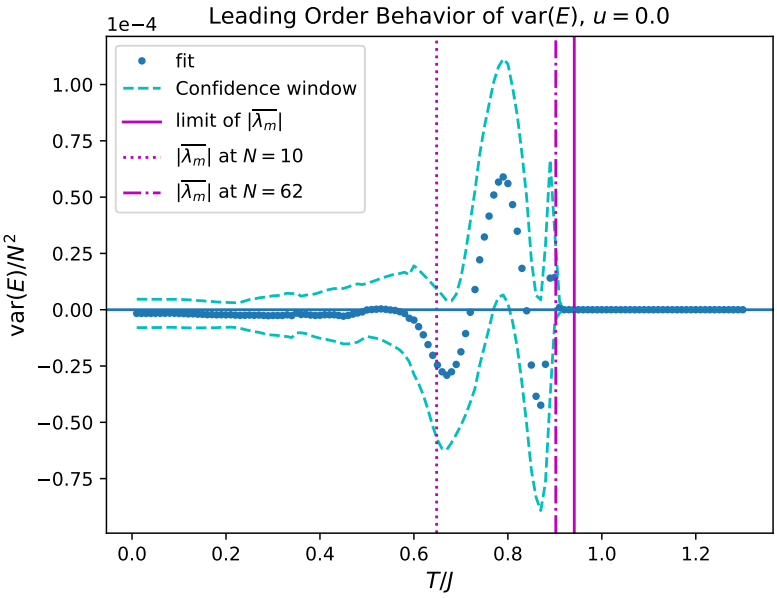

Figure 3.11: Coefficient of N^2 in of E_* regression for $u = 0$, with confidence window.

statistical techniques. Upon being presented with a large number of data points which largely cluster around a zero slope line, there is no statistical basis to expect that the line might suddenly upturn at a later data point or that our knowledge of the slope is likely to be imprecise. This is the problem of induction, not a problem with our analysis.

Finally, before we move on to questions of self-averaging, we briefly discuss the heat capacity (FIG. 3.8). Unfortunately, our data is inconclusive as to whether the average heat capacity will develop a singularity at the limiting value of $\left|\overline{\lambda_m}\right|$ or simply reproduce the discontinuity seen in individual disorder instances. This question is ultimately governed by the N scaling of the $T \to |\lambda_m|^-$ limit of the heat capacity of each individual disorder realization. The authors find this question rather inscrutable based only on Equation A.37 at present. This question might be within the scope of additional numerical attacks of this problem, with higher N and a finer gradation of temperature points.

Our ability to make conclusive statements about self averaging is somewhat weaker

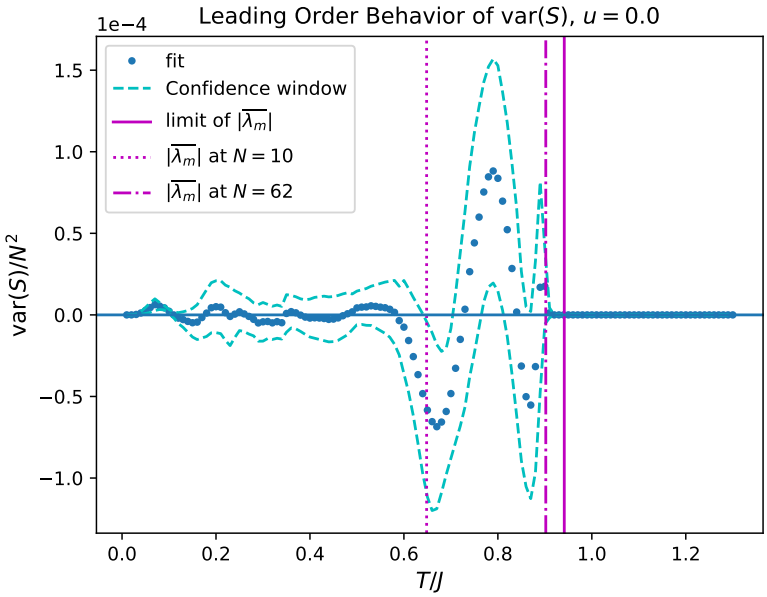

Figure 3.12: Coefficient of N^2 in of S_* regression for $u = 0$, with confidence window.

than our ability to address questions about the averages themselves, unfortunately. We lay the blame here on the slower convergence of the variance estimates of all of our quantities than that of the estimates of their mean. Fortunately, the behavior we do see in the variance estimates looks unambiguously more like noise than signal. Largely, our standard confidence interval includes 0, meaning that we can not reject the hypothesis that these variances are zero with 99% confidence. Even taking into account the fact that some regions of the plots *do* put 0 outside of this confidence interval and that a more modest confidence interval (e.g. 95%) would widen these regions, we still do not find compelling evidence for a lack of self averaging in any of these quantities. Two considerations lead us to this conclusion. Firstly, we find that what estimates we do have for some non-zero $O(N^2)$ component of the variance of some quantity are largely orders of magnitude lower than the $O(N^2)$ component of the square of the mean of this quantity, laying some of the blame at the feet of our inability to detect the full cancellation of two large numbers. Secondly, the behavior of these quantities where they are largest is in

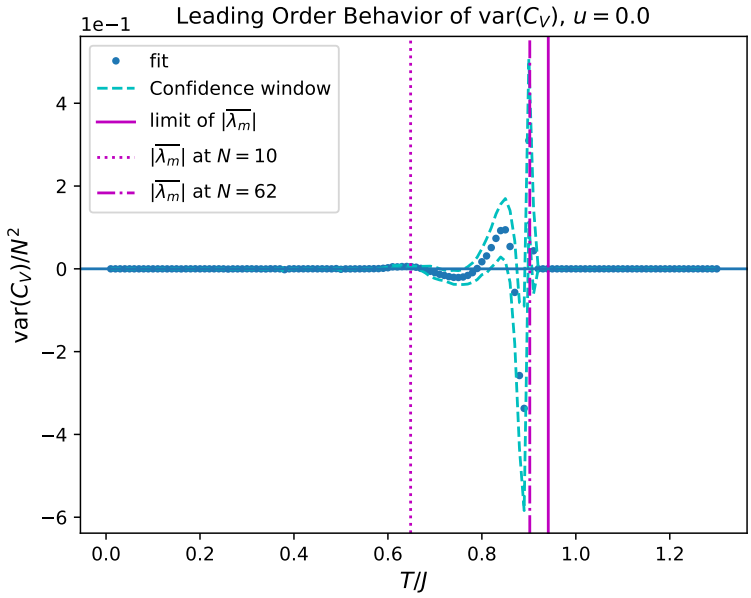

Figure 3.13: Coefficient of N^2 in of C_V regression for $u = 0$, with confidence window.

many cases inconsistent with our physical or statistical expectations. These estimates are occasionally negative, which is impossible for any true leading-order contribution to a variance. Much of the action in these plots is concentrated in the region near the transition, which we have already flagged as a likely haven of finite size effects. Many other regions of concern (e.g. low temperature in FIG. 3.10) occur at temperatures where the fits of the averages show sudden spikes in the size of the confidence window, indicating that these might be driven by errors or outliers.

3.4 Discussion

For the $u > 0$ phase, we have reason to expect that this approximation captures the properties of the time reversal symmetry breaking phase quite well. In fact, as $u \to \infty$ and $T = 0$, the true ground state becomes arbitrarily close to a state in our class of

variational state since (as noted by Bi et al[20])

$$H_u = -\frac{1}{2}\left(\frac{i}{2}\sum_{ij} B_{ij}\eta_i\eta_j\right)^2 \tag{3.75}$$

has a two-fold degenerate ground state spanned by a pair of free Majorana ground states. Indeed, in this limit we can see that $G_* \to \pm f(N)B$ so we expect that the distribution of G_* ought to behave like that of Gaussian random free Majoranas up to some scaling. This expectation is borne out in what numerical results we have, though as we noted we cannot actually fully characterize the distribution of G_* with the moments we have studied. One might express some surprise that $G_* = O(N)$ while $B = O(1)$ (in the sense of norms). However, this is the scaling that one finds in the Gaussian random free Majoranas (set to give an extensive free energy), so this scaling is necessary to prevent the distribution of density matrices from approaching infinite or zero temperature in the $N \to \infty$ limit.

We take a moment to reconcile what might be an apparent difference between our results and those of Bi et al[20], the presence of replica non-diagonal terms in this model. While they find that they can ignore replica indexes in their analysis, they also proceed by considering the boson

$$b = \frac{i}{2}\sum_{ij} B_{ij}\eta_i\eta_j \tag{3.76}$$

which the above argument suggests should behave like $\langle G_*, C_*\rangle$ in its disorder statistics, up to scaling. Using the minimum condition, we can actually identify this quantity with E_*, which self-averages around its first moment according to our analysis. Thus, the replica off-diagonal physics seen in this analysis is simply packaged into their consideration of this boson.

For $u \leq 0$, these results are more a call to action than a conclusive accounting. Since $\lambda_m \to 0$ in this region of parameter space, we are left with the prediction of a phase transition at $T = 0$ into a phase that breaks time reversal symmetry and exhibits some glassy behavior. The particulars of this story should be viewed with a healthy dose of skepticism, since as noted in Section 3.2.4 the variational ground state energy is sub-extensive ($O(\sqrt{N})$) as $N \to \infty$. In particular, this precludes the variational ground state from having an $O(1)$ overlap with the true ground state in this limit.

As an aside, this exposes of a curiosity of this analysis that is perhaps worthy of discussion in its own right: free fermion states are remarkably poor at capturing the physics in this model outside of the $u > 0$ ordered state despite the "average freedom" noted in Section 3.1. One aspect of this is the low overlap of any free fermion ground state with the true ground state at $u \leq 0$ noted above. To the extent that one is willing to interpret an SYK ground state as a generic ground state of a Hamiltonian composed only of interactions, this shows that such states are usually orthogonal to free fermion ground states. We can also see that in the high temperature phase (i.e. the phase with the emergent conformal symmetry) ρ_{t*} self averages around $\rho_{t*} = 2^{-N/2}\mathbb{I}$. That is, in the large N limit, the variational states become certain that they can say precisely nothing about the ensemble of thermal density matrices. One could perhaps argue in their favor that they get the average right, since one can show that an $O(N)$ statistical symmetry of the form possessed by this model forces $\overline{\rho} = 2^{-N/2}\mathbb{I}$. Given that the ensemble of ρ_{t*} must also possess this $O(N)$ symmetry, however, this doesn't argue in their favor above any other $O(N)$ symmetric class of trial states.

With our hammer in hand, however, we take one last swing at that which appears to us a nail. Within the context of this analysis, we expect that while the $T = 0$, $u \leq 0$ phase may break time reversal and exhibit some glassy behavior, it is unlikely to be the same phase as the low temperature $u > 0$ phase. One piece of evidence is actually

the change in scaling of the ground state energy, since this is a rather dramatic change between these two regions of parameter space. We also notice that two $O(N)$ symmetric distributions for G with $\overline{\|G\|^4} = (\overline{\|G\|^2})^2$ need not have the same distribution, in contrast with the case for an $O(N)$ symmetric distribution for an $O(N)$ vector. This is related to the fact mentioned in Section 3.2.3 that the $O(N)$ symmetry begins to fail to constrain the moments of G (or C) to a single scalar starting at the fourth moment. Ultimately, this is due to the fact that the action of $O(N)$ cannot affect the eigenvalues of G beyond permutation.

With this in mind, reviewing the absence of the low temperature feature seen in $\|C_*\|^2$ (FIG. 3.4) for $u = 1$ from the graphs for $u = 0$ and $u = -1$ suggests quite strongly that we are seeing distinct distributions of eigenvalues in the $T \to 0$ limit of G_*. Since the graphs of $\|G_*\|^2$ (FIG. 3.5) all appear roughly identical and to have converged to their $T \to 0$ limit by the time the feature is present in $u = 1$, this feature cannot be due to shifts in the overall size of G_* as a function of temperature. Rather, it suggests that there are some eigenvalues of G_* in the $u = 1$ case that are typically lower than in the $u = 0$ and $u = -1$ case and so are "frozen out" only at lower temperatures. We should be cautious, however, about interpreting this difference as certainly indicating a difference between the $N \to \infty$ limits of these distributions, however, since there are also finite size differences between the two cases. Notably: the $u = 1$ case self averages more slowly, due to the smaller number of components of B relative to J.

In sum, our results represent a tantalizing glimpse into the low temperature physics of the SYK model. We hope that they spark further investigations of the low temperature physics of this model and inform explorations of the non-analyticity predicted at $T = 0$ by the replica calculation.

Appendix A

Supplemental Calculations

A.1 Derivatives of the Trial Free Energy

Our strategy for computing the necessary derivatives will be extending these functions from functions of antisymmetric matrices (thought of as purely imaginary Hermitian matrices) to all Hermitian matrices, using this extension to diagonalize the argument to ease our computation and then restricting the resulting derivatives to act only on antisymmetric matrices. We set our notation to ease determining the domain of any formulas. While we use the notations of ∇ and Hess for the first two derivatives of functions on $\mathcal{A}$ to match the notions on $\mathbb{R}^M$, we will denote the directional derivative of the function $f(X)$ of a Hermitian matrix X at a point X in the directions $\{B_i\}$ by

$$D^n f(X;\{B_i\}) = \left(\prod_i^n \frac{\partial}{\partial \epsilon_i}\right) f\left(X + \sum_i^n \epsilon_i B_i\right)\Bigg|_{\epsilon_i=0} \tag{A.1}$$

where $D^n f(X;\{B_i\})$ of course takes values in the same space that f does (typically, for our purposes, $\mathbb{R}$ or hermitian matrices.) In this context, Df is our notation for the gradient of a scalar function (using the modification of the standard inner product on

Hermitian matrices which restricts to the inner product given in Equation 3.32):

$$\frac{1}{2}\operatorname{Tr}\left[Df(X)Y^{\dagger}\right] = Df(X;Y) \tag{A.2}$$

If f takes values among Hermitian matrices instead, Df will refer to its Jacobian

$$Df(Y)Z = Df(Y;Z) \tag{A.3}$$

Similarly, we write $D^2 f$ to mean the Hessian of a scalar function. That is, $D^2 f = D(Df)$.

There is a natural action of $\Theta \in U(N)$ on all Hermitian matrices by

$$R(\Theta)(X) = \Theta X \Theta^{\dagger} \tag{A.4}$$

Many of our functions will be invariant under this action, so we notice that if $f(R(\Theta)X) = f(X)$ then we have

$$D^n f(R(\Theta)X;\{B_i\}) = D^n f(X;\{R(\Theta^{\dagger})B_i\}) \tag{A.5}$$

Our final ingredient will be a method for taking derivatives of functions defined by Equation 3.23. For this, we notice

$$D^1 X^{-1}(X;B) = -X^{-1}BX^{-1} \tag{A.6}$$

by using the product rule and linearity of scalar derivatives applied to the equation $XX^{-1} = \mathbb{I}$. Applying this to a function of the form given in Equation 3.23 gives

$$D^1 f(X;B) = \frac{1}{2\pi i}\oint_{\gamma} f(z)\left(z\mathbb{I} - X\right)^{-1} B \left(z\mathbb{I} - X\right)^{-1} \mathrm{d}z \tag{A.7}$$

We actually begin with derivatives of $\mathcal{G}$, for reasons which will gradually become clear. Using standard manipulations on free fermion Hamiltonians, we find

$$\mathcal{G} = -\frac{k_B T}{2}\left(N\ln(2) + \mathrm{Tr}\left[\ln\cosh\left(\frac{iG}{k_B T}\right)\right]\right) \tag{A.8}$$

Applying the chain rule, we can actually compute directly with the above technique that for antisymmetric B

$$D^1\mathcal{G}(iG; iB) = -\langle B, C(G)\rangle \tag{A.9}$$

or

$$\nabla_G \mathcal{G} = -C \tag{A.10}$$

We can also compute from our knowledge of free fermions that

$$\langle H_t\rangle_t = -\langle G, C\rangle \tag{A.11}$$

This gives

$$TS = \langle G, D_G\mathcal{G}\rangle - \mathcal{G} \tag{A.12}$$

and, since we will see in a second that $\mathcal{G}$ is concave in G, TS is the Legendre transform of $\mathcal{G}$. Hence,

$$\nabla_C(-TS) = G \tag{A.13}$$

justifying the non-trivial portion of Equation 3.37. We also have

$$T \operatorname{Hess}_C(S) = \operatorname{Hess}_G(\mathcal{G})^{-1} \tag{A.14}$$

allowing us to finish all the derivatives with respect to C that we need once we compute $\operatorname{Hess}_G(\mathcal{G})$. Utilizing Equation A.5, we find

$$\operatorname{Hess}_G(\mathcal{G}) = \tilde{R}(\Phi) P_A R(E) D^2\mathcal{G}(\tilde{G}) R(E^\dagger) P_A^t \tilde{R}(\Phi^t) \tag{A.15}$$

where P_A is the projection from Hermitian matrices to antisymmetric Hermitian matrices,

$$\tilde{G} = \bigoplus_\mu^k \begin{pmatrix} g_\mu & 0 \\ 0 & -g_\mu \end{pmatrix} \tag{A.16}$$

$$E = \frac{1}{\sqrt{2}} \bigoplus_\mu^k \begin{pmatrix} 1 & 1 \\ -i & i \end{pmatrix} \tag{A.17}$$

$$\tilde{R}(\Phi) = P_A R(\Phi) P_A^t \tag{A.18}$$

and Φ "diagonalizes" G in the sense of Section 3.2.1 so that

$$iG = R(\Phi) R(E) \tilde{G} \tag{A.19}$$

On a practical level, we only give formulas for

$$H = P_A R(E) D^2\mathcal{G}(\tilde{G}) R(E^\dagger) P_A^t \tag{A.20}$$

and then recognize that

$$\tilde{R}(\Phi) = \Phi \boxtimes \Phi \tag{A.21}$$

which is sufficient for all of our numerical purposes. Since $\tilde{R}(\Phi)$ is orthogonal, this also allows us to fully characterize the eigenvalues of $\mathrm{Hess}_G(\mathcal{G})$, which is sufficient for all of our analytic arguments.

As for H, a computation using Equation 3.23 and Equation A.6 gives that

$$D^2\mathcal{G}(\tilde{G}; X, Y) = -\frac{1}{2}\sum_{ij} X_{ij}Y_{ji}\frac{w_i - w_j}{h_i - h_j} \tag{A.22}$$

$$w_i = (-1)^{i+1} d_{\lceil \frac{i}{2} \rceil} \tag{A.23}$$

$$h_i = (-1)^{i+1} g_{\lceil \frac{i}{2} \rceil} \tag{A.24}$$

$$\left\lceil \frac{i}{2} \right\rceil = \begin{cases} \frac{i}{2} & i \in 2\mathbb{Z} \\ \frac{i+1}{2} & \text{else} \end{cases} \tag{A.25}$$

After an unpleasant calculation, we can use this to find for $\mu \neq \nu$ and $\epsilon_i = 0$ or 1

$$\left\langle e^{2\mu-1+\epsilon_1, 2\nu-1+\epsilon_2}, He^{2\mu-1+\epsilon_1, 2\nu-1+\epsilon_2} \right\rangle = -D^0_{\mu\nu} - D^1_{\mu\nu} \tag{A.26}$$

$$\left\langle e^{2\mu-1+\epsilon_1, 2\nu-1+\epsilon_2}, He^{2\mu-\epsilon_1, 2\nu-\epsilon_2}) \right\rangle = -(-1)^{\epsilon_1+\epsilon_2}(D^0_{\mu\nu} - D^1_{\mu\nu}) \tag{A.27}$$

$$\left\langle e^{2\mu-1, 2\mu}, He^{2\mu-1, 2\mu} \right\rangle = -\frac{1}{T\cosh^2\left(\frac{g_\mu}{k_B T}\right)} \tag{A.28}$$

where

$$D^\epsilon_{\mu\nu} = \frac{\tanh\left(\frac{g_\mu}{k_B T}\right) - (-1)^\epsilon \tanh\left(\frac{g_\nu}{k_B T}\right)}{g_\mu - (-1)^\epsilon g_\nu} \tag{A.29}$$

and any matrix element left unmentioned is 0. We can see that e^μ is an eigenvector of

H with eigenvalue

$$-\frac{1}{T\cosh^2\left(\frac{g_\mu}{k_BT}\right)} = -\frac{1}{T}\frac{1}{1-d_\mu^2} \tag{A.30}$$

The remaining non-zero matrix elements can be seen by inspection to be block diagonal in the 2×2 blocks

$$\begin{pmatrix} -D^0_{\mu\nu} - D^1_{\mu\nu} & \pm D^0_{\mu\nu} \mp D^1_{\mu\nu} \\ \pm D^0_{\mu\nu} \mp D^1_{\mu\nu} & -D^0_{\mu\nu} - D^1_{\mu\nu} \end{pmatrix} \tag{A.31}$$

which have eigenvalues $-D^0_{\mu\nu}$ and $-D^1_{\mu\nu}$, justifying Equation 3.40 and implicitly completing all analysis of the derivatives of the trial free energy with respect to C.

We need a few modest results about derivatives with respect to G for Section 3.3 and Appendix A.2 which we give now. Using the chain rule, Equation A.10 and Equation 3.37 we find

$$\nabla_G \mathcal{F}_t = -\operatorname{Hess}_G(\mathcal{G})\left(L(C) + G\right) \tag{A.32}$$

which is sufficient for our numerical needs. In the next section, we will also make use of the fact that

$$\begin{aligned} \langle X, \operatorname{Hess}_G(\mathcal{F}_t)Y\rangle = &\langle X, \left(\operatorname{Hess}_G(\mathcal{G})L\operatorname{Hess}_G(\mathcal{G}) - \operatorname{Hess}_G(\mathcal{G})\right)Y\rangle \\ &- D^3\mathcal{G}\left(iG; iX, iY, i(L(C)+G)\right) \end{aligned} \tag{A.33}$$

which can be obtained by differentiating Equation A.32 and making use of the product rule where applicable.

A.2 Specific Heat and Susceptibility Calculations

For the heat capacity, we have

$$C_V = \frac{\partial E_*}{\partial_T} = \left\langle LC_*, \frac{\partial C_*}{\partial T} \right\rangle \tag{A.34}$$

Using the chain rule Equation A.10 gives

$$\frac{\partial C_*}{\partial T} = -\text{Hess}_G(\mathcal{G})_* \left(\frac{\partial G_*}{\partial T} - \frac{G_*}{T} \right) \tag{A.35}$$

while differentiating the minimum condition (Equation 3.38) gives

$$L\left(\frac{\partial C_*}{\partial T} \right) = -\frac{\partial G_*}{\partial T} \tag{A.36}$$

Putting these together, we have

$$C_V = \left\langle G_*, \frac{1}{T}\text{Hess}(\mathcal{G})_* \left(L\text{Hess}(\mathcal{G})_* - \mathbb{I} \right)^{-1} G_* \right\rangle \tag{A.37}$$

For the susceptibility, we add a probe field

$$H_h = -\frac{i}{2} \sum_{ij} h_{ij}\eta_i\eta_j \tag{A.38}$$

and take two derivatives

$$\chi = \text{Hess}_h \, \mathcal{F}_{t*}|_{h=0} \tag{A.39}$$

Since χ is a linear operator $\mathcal{A} \to \mathcal{A}$, its disorder average will be a multiple of the identity

by Schur's lemma:

$$\overline{\chi} = \overline{\chi_0}\mathbb{I} \tag{A.40}$$

where we have defined

$$\chi_0 = \frac{1}{M}\,\mathrm{Tr}\,[\chi] \tag{A.41}$$

Taking one derivative, we see by the chain rule

$$\nabla_h \mathcal{F}_{t*} = C_* + (D_h G_*)^t\, \nabla_G \mathcal{F}_{t*} + (D_h C_*)^t\, h \tag{A.42}$$

where D_h refers to the Jacobian. Using the minimum condition gives, comfortingly,

$$\nabla_h \mathcal{F}_{t*}|_{h=0} = C_* \tag{A.43}$$

Using the minimum condition and chain rule again gives

$$\mathrm{Hess}_h\, \mathcal{F}_{t*}|_{h=0} = (D_h G_*)^t\, \mathrm{Hess}_G\, (\mathcal{F}_t)_*\, D_h G_* - 2\, \mathrm{Hess}_G(\mathcal{G})_* D_h G_* \tag{A.44}$$

At the minimum, Equation A.33 becomes

$$\mathrm{Hess}_G\, (\mathcal{F}_t)_* = \mathrm{Hess}_G(\mathcal{G}) L \mathrm{Hess}_G(\mathcal{G}) - \mathrm{Hess}_G(\mathcal{G}) \tag{A.45}$$

Finally, we note that in the presence of h, the minimum condition shifts to

$$L(C) + G + h = 0 \tag{A.46}$$

Differentiating this with respect to h allows us to see

$$D_h G_* = \left(L \operatorname{Hess}_G(\mathcal{G})_* - \mathbb{I}\right)^{-1} \tag{A.47}$$

which gives, in conjunction with Equation A.44

$$\chi_0 = -\frac{1}{M} \operatorname{Tr}\left[\operatorname{Hess}_G(\mathcal{G})_* \left(L \operatorname{Hess}_G(\mathcal{G})_* - \mathbb{I}\right)^{-1}\right] \tag{A.48}$$

This expression readily exhibits the promised singularity at $T = \lambda_m$ for each individual disorder instance.

Bibliography

[1] D. Ish and L. Balents, *Theory of excitations and dielectric response at a spin-orbital quantum critical point*, *Phys. Rev. B* **92** (Sep, 2015) 094413.

[2] L. Onsager, *Crystal statistics. i. a two-dimensional model with an order-disorder transition*, *Phys. Rev.* **65** (Feb, 1944) 117–149.

[3] A. Altland, P. Altland, and B. Simons, *Condensed Matter Field Theory*. Cambridge University Press, 2006.

[4] L. Mittelstädt, M. Schmidt, Z. Wang, F. Mayr, V. Tsurkan, P. Lunkenheimer, D. Ish, L. Balents, J. Deisenhofer, and A. Loidl, *Spin-orbiton and quantum criticality in* $\mathrm{fesc_2s_4}$, *Phys. Rev. B* **91** (Mar, 2015) 125112.

[5] N. J. Laurita, J. Deisenhofer, L. Pan, C. M. Morris, M. Schmidt, M. Johnsson, V. Tsurkan, A. Loidl, and N. P. Armitage, *Singlet-triplet excitations and long range entanglement in the spin-orbital liquid candidate FeSc2S4*, *ArXiv e-prints* (Oct., 2014) [arXiv:1410.6777].

[6] G. Kalvius, O. Hartmann, D. Noakes, F. Wagner, R. Wäppling, U. Zimmermann, C. Baines, A. Krimmel, V. Tsurkan, and A. Loidl, *A μsr magnetic study of frustrated fesc2s4 and mnsc2s4*, *Physica B: Condensed Matter* **378** (2006) 592–593.

[7] N. Büttgen, A. Zymara, C. Kegler, V. Tsurkan, and A. Loidl, *Spin and orbital frustration in fesc 2 s 4 probed by sc 45 nmr*, *Physical Review B* **73** (2006), no. 13 132409.

[8] A. Krimmel, M. Mücksch, V. Tsurkan, M. M. Koza, H. Mutka, and A. Loidl, *Vibronic and magnetic excitations in the spin-orbital liquid state of* $\mathrm{fesc_2s_4}$, *Phys. Rev. Lett.* **94** (Jun, 2005) 237402.

[9] V. Fritsch, J. Hemberger, N. Büttgen, E.-W. Scheidt, H.-A. Krug von Nidda, A. Loidl, and V. Tsurkan, *Spin and orbital frustration in* $\mathrm{mnsc_2s_4}$ *and* $\mathrm{fesc_2s_4}$, *Phys. Rev. Lett.* **92** (Mar, 2004) 116401.

[10] N. Bttgen, J. Hemberger, V. Fritsch, A. Krimmel, M. Mcksch, H.-A. K. von Nidda, P. Lunkenheimer, R. Fichtl, V. Tsurkan, and A. Loidl, *Orbital physics in sulfur*

spinels: ordered, liquid and glassy ground states, *New Journal of Physics* **6** (2004), no. 1 191.

[11] G. Chen, A. P. Schnyder, and L. Balents, *Excitation spectrum and magnetic field effects in a quantum critical spin-orbital system: The case of* $fesc_2s_4$, *Phys. Rev. B* **80** (Dec, 2009) 224409.

[12] G. Chen, L. Balents, and A. P. Schnyder, *Spin-orbital singlet and quantum critical point on the diamond lattice:* $\mathrm{fesc}_2\mathbf{s}_4$, *Phys. Rev. Lett.* **102** (Mar, 2009) 096406.

[13] G. A. Slack, S. Roberts, and F. S. Ham, *Far-infrared optical absorption of* fe^{2+} *in zns*, *Phys. Rev.* **155** (Mar, 1967) 170–177.

[14] J. T. Vallin, G. A. Slack, and C. C. Bradley, *Far-infrared absorption of zns:*fe^{2+} *in strong magnetic fields*, *Phys. Rev. B* **2** (Dec, 1970) 4406–4413.

[15] S. Sarkar, T. Maitra, R. Valentí, and T. Saha-Dasgupta, *Comparative study of* $fecr_2s_4$ *and* $fesc_2s_4$*: Spinels with orbitally active a site*, *Phys. Rev. B* **82** (Jul, 2010) 041105.

[16] S. Sachdev, *Bekenstein-hawking entropy and strange metals*, *Phys. Rev. X* **5** (Nov, 2015) 041025.

[17] A. Kitaev, *A simple model of quantum holography*, *Talks given at the KITP program: Entanglement in Strongly Correlated Quantum Matter, April 7 and May 27* (2015).

[18] J. Maldacena and D. Stanford, *Remarks on the sachdev-ye-kitaev model*, *Phys. Rev. D* **94** (Nov, 2016) 106002.

[19] J. Polchinski and V. Rosenhaus, *The spectrum in the sachdev-ye-kitaev model*, *Journal of High Energy Physics* **2016** (Apr, 2016).

[20] Z. Bi, C.-M. Jian, Y.-Z. You, K. A. Pawlak, and C. Xu, *Instability of the non-fermi-liquid state of the sachdev-ye-kitaev model*, *Phys. Rev. B* **95** (May, 2017) 205105.

[21] S. F. Edwards and P. W. Anderson, *Theory of spin glasses*, *Journal of Physics F: Metal Physics* **5** (1975), no. 5 965.

[22] E. Marinari, G. Parisi, F. Ricci-Tersenghi, J. J. Ruiz-Lorenzo, and F. Zuliani, *Replica symmetry breaking in short-range spin glasses: Theoretical foundations and numerical evidences*, *Journal of Statistical Physics* **98** (Mar, 2000).

[23] T. Tao, *Topics in Random Matrix Theory*. Graduate studies in mathematics. American Mathematical Soc., 2012.

[24] H. White, *A heteroskedasticity-consistent covariance matrix estimator and a direct test for heteroskedasticity*, *Econometrica* **48** (1980), no. 4.